

# Reference prior for Bayesian estimation of seismic fragility curves

Antoine Van Biesbroeck<sup>a,b,\*</sup>, Clément Gauchy<sup>c</sup>, Cyril Feau<sup>b</sup>, Josselin Garnier<sup>a</sup>

<sup>a</sup>CMAP, CNRS, École polytechnique, Institut Polytechnique de Paris, 91120 Palaiseau, France

<sup>b</sup>Université Paris-Saclay, CEA, SEMT, 91191 Gif-sur-Yvette, France

<sup>c</sup>Université Paris-Saclay, CEA, SGLS, 91191 Gif-sur-Yvette, France

---

## Abstract

One of the crucial quantities of probabilistic seismic risk assessment studies is the fragility curve, which represents the probability of failure of a mechanical structure conditional to a scalar measure derived from the seismic ground motion. Estimating such curves is a difficult task because for most structures of interest, few data are available, whether they come from complex numerical simulations or experimental campaigns. For this reason, a wide range of the methods of the literature rely on a parametric log-normal model. Bayesian approaches allow for efficient learning of the model parameters. However, for small data set sizes, the choice of the prior distribution has a non-negligible influence on the posterior distribution, and therefore on any resulting estimate. We propose a thorough study of this parametric Bayesian estimation problem when the data are binary (i.e. data indicate the state of the structure, failure or non-failure). Using the reference prior theory as a support, we suggest an objective approach for the prior choice to simulate a posteriori fragility curves. This approach leads to the Jeffreys prior and we prove that this prior depends only of the ground motion characteristics, making its calculation suitable for any equipment in an industrial installation subjected to the same seismic hazard. Our proposal is theoretically and numerically compared to those classically proposed in the literature by considering three different case studies. The results show the robustness and advantages of the Jeffreys prior in terms of regularization (no degenerate estimations) and stability (no outliers of the parameters) for fragility curves estimation.

*Keywords:* Bayesian analysis, Fragility curves, Reference prior, Jeffreys prior, Seismic Probabilistic Risk Assessment

---

## 1. Introduction

Seismic fragility curves of mechanical structures are key quantities of interest of the Seismic Probabilistic Risk Assessment (SPRA) framework. They are introduced in the 1980s for seismic risk assessment studies performed on nuclear facilities (see e.g. [1–5]). They express the probability of failure of the mechanical structure – the probability that an Engineering Demand Parameter (EDP), such as interstory drift ratio for example, exceeds a limit threshold whether the EDP is observed or not – conditional to a scalar value derived from the seismic ground motions – coined Intensity Measure (IM) – such as Peak Ground Acceleration (PGA). In [5], Cornell recalls the main assumption according to which the reduction of the seismic hazard to the IM values is relevant. This is the so-called sufficiency assumption of the IM w.r.t. the magnitude (M), source-to-site distance (R) and other parameters thought to dominate the seismic hazard at the location of interest (see also [6]). Fragility curves are also part of the Performance-Based Earthquake Engineering (PBEE) framework (see e.g. [5, 7–9]). In this context, they are based on an alternative definition, the probability of exceeding a specified damage state for a given EDP.

Various data sources can be exploited in practice to estimate fragility curves, namely: expert judgments supported by test data [1–3, 10], experimental data [3, 9, 11], results of damage – called empirical data – collected on existing

---

\*Corresponding author

*Email addresses:* antoine.van-biesbroeck@polytechnique.edu (Antoine Van Biesbroeck), clement.gauchy@cea.fr (Clément Gauchy), cyril.feau@cea.fr (Cyril Feau), josselin.garnier@polytechnique.edu (Josselin Garnier)

structures that have been subjected to an earthquake [12–14] and analytical results given by more or less refined numerical models using artificial or real seismic excitations (see e.g. [15–20]).

Parametric fragility curves were historically introduced in the SPRA framework because their estimates require small sample sizes. The log-normal model has since become the most widely used model (see e.g. [12–25]). In practice several strategies can be implemented to fit the two parameters of the model namely, the median,  $\alpha$ , and the log standard deviation,  $\beta$ . When the data are binary (i.e. failure or not failure), [13] recommend the Maximum Likelihood Estimation (MLE). This technique is itself one of the most used. When the data are independent, the bootstrap technique is additionally used to obtain confidence intervals relating to the size of the sample considered (e.g. [12, 15, 16]). When the data-set contains more information than the failure indications, for instance, when the failure of the mechanical structure happens when an EDP exceeds a limit threshold and the EDP is observed, techniques based on machine learning can also be exploited such as: linear regression or generalized linear regression [13], classification - based techniques [26–28], kriging [29–31], polynomial chaos expansion [32], Artificial Neural Networks (ANN) [18, 19, 33]. When data come from numerical simulations, some of these methods can be coupled with adaptive techniques to reduce the number of calculations to be performed [19, 28, 29, 34]. Some of these techniques are compared in [13] highlighting advantages and disadvantages.

The Bayesian framework has recently become increasingly popular in seismic fragility analysis (see e.g. [9, 19, 25, 35–40]). It actually allows to solve the irregularity issues encountered for the estimation of the parametric fragility curves, by using for example the MLE-based method which can lead to unrealistic or degenerate fragility curves such as unit step functions, when the data availability is sparse. Those problems are especially encountered when resorting to complex and detailed modeling – or high-fidelity models – due to the calculation burden or when dealing with tests performed on shaking tables, etc. In earthquake engineering, Bayesian inference is often used to update log-normal fragility curves obtained beforehand by various approaches, by assuming independent distributions for the prior values of  $(\alpha, \beta)$  such as log-normal distributions for instance. For instance, in [37] and [38], the median prior values come from equivalent linearized mechanical models. In [19], the aleatory and epistemic uncertainties are both taken into account in the parametric model initially introduced in [1]. An ANN is trained and used to characterize (i) the aleatory uncertainty and (ii) the prior median value of  $\alpha$  whereas its associated epistemic uncertainty is taken from literature. The log-normal prior distribution of  $\alpha$  is then updated with empirical data. In [25], results of Incremental Dynamic Analysis are used to obtain a prior value of  $\alpha$  whereas a parametric study is carried out to determine the prior value of  $\beta$  which leads to a satisfactory convergence whatever its target value, before application to practical problems. In [14], [Straub and Der Kiureghian](#) mainly focus on consequences of statistical dependencies in the data on fragility analyses. The prior is defined as the product of a normal distribution for  $\ln(\alpha)$  and the improper distribution  $1/\beta$  for  $\beta$ . The normal distribution is defined based on engineering judgment assuming that, for the component of interest for example, the median lies between 0.02 g and 3 g with 90% probability. This prior was preferred to  $1/\alpha$  on the grounds that it led to unrealistically large posterior values of  $\alpha$ . A sensitivity analysis is further performed to examine the influence of the choice of the prior distribution on the final results. The Bayesian framework is also relevant to fit numerical models – e.g. mathematical expressions based on engineering judgments or physics-based models – to experimental data to estimate the fragility curves [9, 40], or metamodels such as logistic regressions [35, 39].

In this paper, we only deal with binary data within a Bayesian framework. The Bayesian standpoint is considered by focusing on the influence of the prior on the estimates of the fragility curves, as part of the SPRA. With a small data set, the choice of the prior has indeed a non-negligible influence on the posterior distribution and therefore on the estimation of any quantity of interest related to the fragility curves. Thus, besides the simulation-based approaches, this paper also addresses the problems of equipment for which only results of qualification tests are available, such as electrical devices (e.g. relays, etc.) or complex structures such as free-standing stacked structures, etc. So, in this work, the purpose is, as much as possible, to choose the prior by removing any subjectivity which can rightfully lead to inevitable open questions about the influence of the prior on the final results. By relying on the reference prior theory, which defines relevant metrics to express whether a prior can be called "objective" [41], we focus on the well-known Jeffreys prior, asymptotic optimum of the mutual information w.r.t. the dataset size [42]. Of course, in this context, there remains the choice of the parametric model – which is here the log-normal model – for the fragility curves. However, numerical experiments based on the seismic responses of simple mechanical systems – i.e. few degrees of freedom mechanical systems – suggest that the choice of an appropriate IM makes it possible to reduce the potential biases between reference fragility curves – that can be obtained by Monte-Carlo simulations – and their lognormal estimates (see e.g. [34]).

After a statement of the problem under the Bayesian point of view in the next section, we review the objective prior theory and its main results in section 3. Our main contributions start in section 4 where the reference prior is properly computed and estimated for the issue of concern. In section 5, the estimation tools and the performance evaluation metrics used in this work are presented. They are implemented in section 6 on three different case studies. For each case, the *a posteriori* distributions of the parameters of the log-linear probit model and of the corresponding fragility curves are compared with those obtained with classical a priori choices taken from the literature. As main results of this work, we theoretically and numerically demonstrate the robustness and advantages of the Jeffreys prior in terms of regularization (no degenerate estimations) and stability (no outliers of the parameters) for fragility curves estimations. Finally, to close this paper, a conclusion is proposed in section 7.

## 2. Bayesian problem

As mentioned in the introduction, a log-linear probit model is often used to approximate fragility curves. In this model the probability of failure given the IM takes the following form:

$$P_f(a) = \mathbb{P}(\text{'failure'} | \text{IM} = a) = \Phi\left(\frac{\log a - \log \alpha}{\beta}\right), \quad (1)$$

where  $\alpha, \beta \in (0, +\infty)$  are the two model parameters and  $\Phi$  is the cumulative distribution function of a standard Gaussian variable. In the following we denote  $\theta = (\alpha, \beta)$ . In the Bayesian point of view  $\theta$  is considered as a random variable [43]. Its distribution is denoted by  $\pi$  and called the prior, it is supposed to be defined on a set  $\Theta \subset (0, +\infty)^2$ .

Our statistical model consists into the observations of independent realizations  $(a_1, z_1), \dots, (a_k, z_k) \in \mathcal{A} \times \{0, 1\}$ ,  $\mathcal{A} \subset [0, \infty)$ ,  $k$  being the data-set size. For the  $i$ th seismic event,  $a_i$  is its observed IM and  $z_i$  is the observation of a failure ( $z_i$  is equal to one if failure has been observed during the  $i$ th seismic event and it is equal to zero otherwise). The joint distribution of the pair  $(a, z)$  conditionally to  $\theta$  has the form:

$$p(a, z | \theta) = p(a)p(z | a, \theta), \quad (2)$$

where  $p(a)$  denotes the distribution of the IM and  $p(z | a, \theta)$  is a Bernoulli distribution whose parameter (the probability of failure) depends on  $a$  and  $\theta$  as expressed by equation (1). The product of the conditional distributions  $p(z_i | a_i, \theta)$  is the likelihood of our model and is expressed as

$$\ell_k(\mathbf{z} | \mathbf{a}, \theta) = \prod_{i=1}^k \Phi\left(\frac{\log \frac{a_i}{\alpha}}{\beta}\right)^{z_i} \left(1 - \Phi\left(\frac{\log \frac{a_i}{\alpha}}{\beta}\right)\right)^{1-z_i}, \quad (3)$$

denoting  $\mathbf{a} = (a_i)_{i=1}^k$ ,  $\mathbf{z} = (z_i)_{i=1}^k$ .

The *a posteriori* distribution of  $\theta$  can be computed by Bayes theorem. The resulting distribution

$$p(\theta | \mathbf{a}, \mathbf{z}) = \frac{\ell_k(\mathbf{z} | \mathbf{a}, \theta)\pi(\theta)}{\int_{\Theta} \ell_k(\mathbf{z} | \mathbf{a}, \theta')\pi(\theta')d\theta'} \quad (4)$$

is called the posterior. Sampling  $\theta$  with the posterior distribution allows for the estimation of any quantity of interest. This method is explained further in section 5.2. Note that the Bayesian method requires the choice of the prior  $\pi$ . Such a choice without any subjectivity is the subject of the next section.

## 3. Reference prior theory

This section is devoted to the choice of the prior in the Bayesian context. To this end, we deal with the notion of mutual information. Its definition and its usefulness in Bayesian problems is not new [41, 44], however, its use to estimate seismic fragility curves has not yet been studied in the literature. Shannon's information theory provides relevant elements for this problem. Information entropy is a common example that helps distinguish between an informative or non-informative distribution [45].

One way to define a non-subjective prior is to look for a non-informative one (i.e. with high entropy). However, this type of prior leads to a posterior distribution little influenced by the likelihood of the statistical model and can lead to unrealistic posterior values of the parameters of interest when little data is available. The consequence is then a weaker convergence of the resulting estimates. Moreover, in practice, in earthquake engineering in particular, we note that it is difficult to completely define a prior by a “rigorous” approach. For a given distribution for example – which is already a subjective choice that is not always easy to justify – the median can be obtained beforehand via a less refined mechanical model. There remains, however, the question of the choice of the associated variance, of which we have just said that the consequences on the convergence of the *a posteriori* estimates are not negligible. For all these reasons, the search for an *a priori* with objective information is relevant.

To choose such a prior, we consider the criterion introduced by Bernardo [44] to define the so-called reference priors. It consists in choosing the prior that maximizes the mutual information indicator  $I(\pi|k)$  which expresses the information provided by the data to the posterior, relatively to the prior. In other words, this criterion seeks the prior that maximizes the “learning” capacity from observations. The mutual information indicator is defined by:

$$I(\pi|k) = \int_{(\mathcal{A} \times \{0,1\})^k} KL(p(\cdot|\mathbf{a}, \mathbf{z})|\pi)p(\mathbf{a}, \mathbf{z}) \prod_{l=1}^k \lambda(da_l, dz_l), \quad (5)$$

where the reference measure  $\lambda$  is the product of the Lebesgue measure over  $\mathcal{A}$  w.r.t.  $a$  and the discrete measure  $\delta_0 + \delta_1$  over  $\{0, 1\}$  w.r.t.  $z$ . This indicator is based on the Kullback-Leibler divergence between the posterior and the prior, which is known to numerically express this idea of the information provided by one distribution to another one:

$$KL(p||q) = \int_{\Theta} p(\theta) \log \frac{p(\theta)}{q(\theta)} d\theta. \quad (6)$$

A suitable definition of a reference prior is suggested in the literature as the solution of an asymptotic optimization of this mutual information metric [42, 46]. It has been proved that, under some mild assumptions which are satisfied in our framework, the Jeffreys prior defined by

$$J(\theta) \propto \sqrt{|\det I^k(\theta)|}, \quad (7)$$

is the reference prior, with  $I^k$  being the Fisher information matrix:

$$I(\theta)_{i,j}^k = - \int_{(\mathcal{A} \times \{0,1\})^k} \ell_k(\mathbf{z}|\mathbf{a}, \theta) \frac{\partial^2 \log \ell_k(\mathbf{z}|\mathbf{a}, \theta)}{\partial \theta_i \partial \theta_j} \prod_{l=1}^k p(a_l) \lambda(da_l, dz_l). \quad (8)$$

The property  $I(\theta)^k = kI(\theta)$  makes  $J$  independent of  $k$ , as its definition only stands up to a multiplicative constant. The Jeffreys prior is already well known in Bayesian theory for being invariant by a reparametrization of the statistical model [47]. This property is essential as it makes the choice of the model parameters  $\theta$  without any incidence on the resulting posterior.

#### 4. Jeffreys prior construction

According to the previous discussion, the Jeffreys prior seems to be the best objective prior candidate for our problem. Thus, in this section, we carry out its calculation to estimate log-normal seismic fragility curves with binary data. The application of the reference prior theory to this field of study is, to our knowledge, new.

##### 4.1. Jeffreys prior calculation

In a first step, we compute the Fisher information matrix  $I(\theta) = I(\theta)^1$  in our model. Here,  $\theta = (\alpha, \beta) \in \Theta$  and

$$I(\theta)_{i,j} = - \int_{\mathcal{A} \times \{0,1\}} p(z|a, \theta) \frac{\partial^2 \log p(z|a, \theta)}{\partial \theta_i \partial \theta_j} p(a) \lambda(da, dz) \quad (9)$$

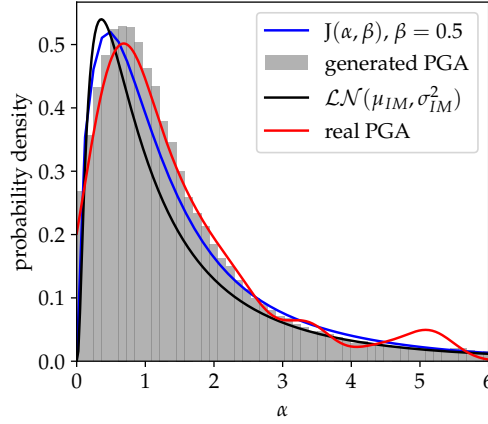


Figure 1: Comparison of a sectional view of the Jeffreys prior w.r.t.  $\alpha$  (blue line) with some PGA distributions: approximated distribution of real accelerograms via Gaussian kernels in red, histogram of the generated signals in gray, and log-normal fit of the distribution in black.

for  $i, j \in \{1, 2\}$ , with  $p(z|a, \theta) = \ell_1(z|a, \theta)$  being the likelihood expressed in equation (3), i.e.

$$\log p(z|a, \theta) = z \log \Phi\left(\frac{\log a - \log \alpha}{\beta}\right) + (1 - z) \log \left(1 - \Phi\left(\frac{\log a - \log \alpha}{\beta}\right)\right). \quad (10)$$

From this expression, after a formal derivation of the partial derivative of  $\log p(z|a, \theta)$ , the Fisher information matrix is computed numerically, from approximations of the integrals over  $\mathcal{A}$ . See [Appendix A](#) for more details.

#### 4.2. Practical implementation

Section 3 shows that the probability distribution of the IM is necessary to calculate the Fisher information matrix. Without loss of generality regarding the applicability of the methodology, we consider in the following the PGA as IM. In this work we use  $10^5$  artificial seismic signals generated using the stochastic generator defined in [48] and implemented in [28] from 97 real accelerograms selected in the European Strong Motion Database for  $5.5 \leq M \leq 6.5$  and  $R < 20$  km. Enrichment is not a necessity in the Bayesian framework – especially if we have a sufficient number of real signals – but it allows comparisons with the reference method of Monte-Carlo for simulation-based approaches as well as comparative studies of performance. Note that the synthetic signals have the same PGA distribution as the real ones, as shown in Figure 1.

In practice, due to the use of Markov Chain Monte Carlo (MCMC) methods (see section 5.2) to sample the *a posteriori* distribution, the prior must be evaluated (up to a multiplicative constant) many times in the calculations. Because of its computational complexity due to the integrals to be computed, we decided to perform evaluations of the prior on an experimental design based on a fine-mesh grid of  $\Theta$  (here  $[0, \infty)^2$ ) and to build an interpolated approximation of the Jeffreys prior from this design. This strategy is more suitable for our numerical applications and very tractable because the domain  $\Theta$  is only two-dimensional. Figure 2 gives a plot of the Jeffreys prior. To be precise,  $500 \times 500$  prior values have been computed for  $\alpha \in [10^{-5}, 10]$  and  $\beta \in [10^{-3}, 2]$ . A linear interpolation has been processed from these.

#### 4.3. Discussion

The computational complexity of the Jeffreys prior is not in itself a major drawback. Depending solely on the distribution of the IM, its initial calculation will quickly be valued at the scale of an installation such as a nuclear plant which comprises several Structures and Components (SCs) whose fragility curves must be evaluated. Compared to methodologies that aim to define a prior on the basis of prior mechanical calculations which are specific to SCs by definition, the advantage of the Jeffreys prior is its generic character as will be seen in the applications section of this paper (section 6). Moreover, this prior is completely defined, it does not depend on an additional subjective choice.

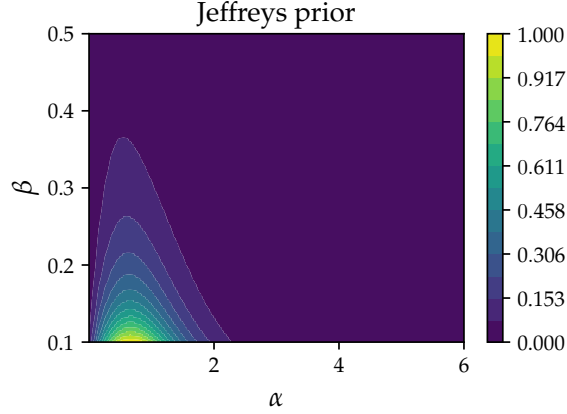


Figure 2: The Jeffreys prior calculated from PGA and plotted in the subdomain  $[0, 6] \times [0.1, 0.5]$ .

The Jeffreys prior is known to be improper in numerous common cases (i.e. it cannot be normalized as a probability). In the present case, its asymptotic behavior is computed for different limits of  $\theta = (\alpha, \beta)$  in [Appendix B](#) which shows that it is indeed improper. This characteristic is not an issue, as our work focuses on the posterior which is proper as proved in [Appendix B](#). This property is essential as MCMC algorithms would not make any sense if the posterior were improper. These asymptotic expansions also provide complementary and essential insight into the Jeffreys prior. They make it possible to understand that its behavior in  $\alpha$  is similar to that of a log-normal distribution having the same median as that of the IM (i.e. here 1.1 m/s<sup>2</sup>) with a variance which is the sum of the variance of the IM and of a term which depends on  $\beta$ . [Figure 1](#) clearly illustrates this result.

## 5. Estimation tools, competing approaches and performance evaluation metrics

In this section, we first present the Bayesian estimation tools and the Monte-Carlo reference method to which we refer to evaluate the relevance of the log-normal model when the number of data allows it. Then, to evaluate the performance of the Jeffreys prior on practical cases, we present two competing approaches that we implement. On the one hand, we apply the MLE method widely used in literature, coupled with a bootstrap technique. On the other hand, we apply a Bayesian technique implemented with the prior introduced by [Straub and Der Kiureghian \[14\]](#). For a fair comparison we propose to calibrate the latter according to the results of [Figure 1](#) which evinces that in  $\alpha$  the distribution is similar to the PGA distribution of the synthetic and real signals. It would indeed be easy to calibrate it in such a way so as to skew comparisons, by considering, for instance, a too large variance. Finally, performance evaluation metrics are defined.

### 5.1. Fragility curves estimations via Monte-Carlo

Here we assume that a validation data-set  $(\mathbf{a}^{\text{MC}}, \mathbf{z}^{\text{MC}}) = ((a_i^{\text{MC}})_{i=1}^{N^{\text{MC}}}, (z_i^{\text{MC}})_{i=1}^{N^{\text{MC}}})$  is available and this section describes how from such a large data-set a fragility curve can be obtained by nonparametric estimation that can serve as a reference from which our estimations (based on a small data-set and parametric estimation) can be compared.

Good candidates are Monte-Carlo (MC) estimators which estimate the expected number of failures locally w.r.t. the IM. We first need to define a subdivision of the IM values and to estimate the failure probability on each of the sub-intervals. Regular subdivisions are not appropriate because the observed IMs are not uniformly distributed. We follow the suggestion by [Trevlopoulos et al. \[24\]](#) to take clusters of the IM using K-means. Given such  $N_c$  clusters  $(K_j)_{j=1}^{N_c}$ , the Monte-Carlo fragility curve estimated at the centroids  $(c_j)_{j=1}^{N_c}$  is expressed as

$$P_f^{\text{MC}}(c_j) = \frac{1}{n_j} \sum_{i, a_j^{\text{MC}} \in K_j} z_j^{\text{MC}}, \quad (11)$$

where  $n_j$  is the sample size of cluster  $K_j$ . An asymptotic confidence interval for this estimator can also be derived using its Gaussian approximation. It is accepted that a MC-based fragility curve is a reference curve because it is not based on any assumption.

## 5.2. Fragility curves estimations in the Bayesian framework

To benefit from the Bayesian theory introduced in section 3 and the reference prior construction presented in section 4, the relevant method is to derive the posterior defined in equation (4) and to generate, according to that distribution, samples of  $\theta$  conditioned on the observed data. Those *a posteriori* generations of  $\theta$  can be performed thanks to MCMC methods. We have implemented an adaptive Metropolis-Hastings (M-H) algorithm with Gaussian transition kernel and covariance adaptation [49]. Such an algorithm allows simulations from a probability density known up a multiplicative constant. In this context, the *a posteriori* samples of  $\theta$  can be used to define credibility intervals for the log-normal estimates of the fragility curves.

## 5.3. Competing approaches for performance evaluation

### 5.3.1. Multiple MLE by bootstrapping

The best known parameter estimation method is the MLE, defined as the maximal argument of the likelihood derived from the observed data:

$$\hat{\theta}_k^{\text{MLE}} = \arg \max_{\theta \in \Theta} \ell_k(\mathbf{z}|\mathbf{a}, \theta). \quad (12)$$

A common method for obtaining a wide range of  $\theta$  estimates is to compute multiple MLE by bootstrapping. Denoting the data-set size by  $k$ , bootstrapping consists in doing  $L$  independent draws with replacement of  $k$  items within the data-set. Those lead to  $L$  different likelihoods from the  $k$  initial observations, and so to  $L$  values of the estimator which can be averaged. In the context of fragility curves, this method is widespread (see e.g. [12, 13, 16, 50, 51]). The convergence of the MLE and the relevance of this method is stated in [52]. Nevertheless the bootstrap method is often limited by the irregularity of the results for small values of  $k$  (see e.g. [10]). In this context, the  $L$  values of  $\theta$  are used to define confidence intervals for the log-normal estimates of the fragility curves.

### 5.3.2. Prior suggested by Straub and Der Kiureghian [14]

The prior suggested by Straub and Der Kiureghian – called SK’s prior – is defined as the product of a normal distribution for  $\ln(\alpha)$  and the improper distribution  $1/\beta$  for  $\beta$ , namely:

$$\pi_{SK}(\theta) \propto \frac{1}{\alpha\beta} \exp\left(-\frac{(\log \alpha - \mu)^2}{2\sigma^2}\right). \quad (13)$$

In [14] the parameters  $\mu$  and  $\sigma$  of the log-normal distribution are chosen to generate a non-informative prior. As specified in the introduction to section 5, for a fair comparison with the approach proposed in this paper, we decided to choose  $\mu$  and  $\sigma$  being equal to the mean and the standard deviation of the logarithm of the IM. This choice is consistent with the fact that the Jeffreys prior is similar to a log-normal distribution with these parameters (see Figure 1). The prior  $\pi_{SK}(\theta)$  is plotted in Figure 3.

An analysis of the posterior which results from SK’s prior is given in Appendix B. It shows that the posterior is improper. This statement jeopardizes the validity of any *a posteriori* simulations using MCMC methods. This issue is nevertheless manageable with the consideration of a truncation w.r.t.  $\beta$ . In Appendix C we verify that the same issue still stands within the authors’ original framework which is slightly different from ours.

## 5.4. Performance evaluation metrics

To have a clear view of the performance of the proposed approach, we consider two quantitative metrics which can be calculated for each of the methods described in section 5.3. We consider the sample  $(\mathbf{a}, \mathbf{z})$ . We denote by  $a \mapsto P_f^{\mathbf{a}, \mathbf{z}}(a)$  the random process defined as the fragility curve conditional to the sample (the probability distribution of  $P_f^{\mathbf{a}, \mathbf{z}}(a)$  is inherited from the *a posteriori* distribution of  $\theta$ ). For each value  $a$  the  $r$ -quantile of the random variable  $P_f^{\mathbf{a}, \mathbf{z}}(a)$  is denoted by  $q_r^{\mathbf{a}, \mathbf{z}}(a)$ . We define:

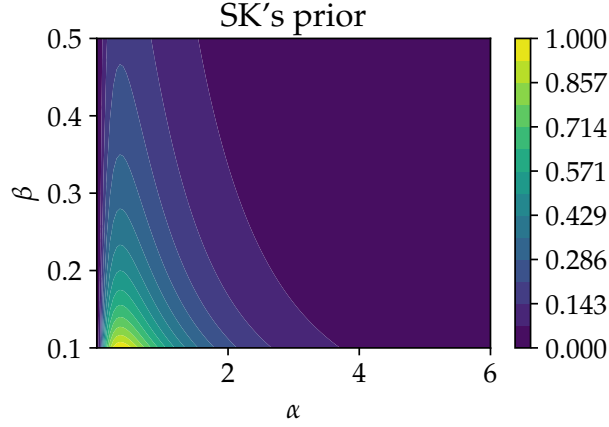


Figure 3: Prior suggested by [Straub and Der Kiureghian \[14\]](#) and plotted in the subdomain  $[0, 6] \times [0.1, 0.5]$ . It is expressed in equation (13) and scaled on a log-normal estimation of the PGA's distribution.

- The conditional quadratic error:

$$\mathcal{E}^{Q|\mathbf{a}, \mathbf{z}} = \mathbb{E}[\|P_f^{\mathbf{a}, \mathbf{z}} - P_f^{\text{MLE}}\|_{L^2}^2 | \mathbf{a}, \mathbf{z}] = \int_0^{A_{\max}} \mathbb{E}[(P_f^{\mathbf{a}, \mathbf{z}}(a) - P_f^{\text{MLE}}(a))^2 | \mathbf{a}, \mathbf{z}] da. \quad (14)$$

$P_f^{\text{MLE}}$  stands for the log-normal estimate of the fragility curve obtained by MLE (see section 5.1) with all the database available according to the case study. We further check that this estimate is close to the reference curve obtained by MC when possible (see section 6).

- The conditional width of the  $1 - r$  credibility zone for the fragility curve:

$$\mathcal{S}^{r|\mathbf{a}, \mathbf{z}} = \|q_{1-r/2}^{\mathbf{a}, \mathbf{z}} - q_{r/2}^{\mathbf{a}, \mathbf{z}}\|_{L^2}^2 = \int_0^{A_{\max}} (q_{1-r/2}^{\mathbf{a}, \mathbf{z}}(a) - q_{r/2}^{\mathbf{a}, \mathbf{z}}(a))^2 da. \quad (15)$$

To estimate such variables, we simulate a set of  $L$  fragility curves  $(P_f^{\theta_i|\mathbf{a}, \mathbf{z}})_{i=1}^L$  where  $(\theta_i)_{i=1}^L$  is a sample of the *a posteriori* distribution of the model parameters obtained by MCMC. The empirical quantiles  $\hat{q}_r^{\theta_i|\mathbf{a}, \mathbf{z}}(a)$  of  $(P_f^{\theta_i|\mathbf{a}, \mathbf{z}}(a))_{i=1}^L$  are approximations of the quantiles  $q_r^{\mathbf{a}, \mathbf{z}}(a)$  of the random variable  $P_f^{\mathbf{a}, \mathbf{z}}(a)$ . We derive

- The approximated conditional quadratic error:

$$\hat{\mathcal{E}}_L^{Q|\mathbf{a}, \mathbf{z}} = \frac{1}{L} \sum_{i=1}^L \|P_f^{\theta_i|\mathbf{a}, \mathbf{z}} - P_f^{\text{MLE}}\|_{L^2}^2. \quad (16)$$

- The approximated conditional width of the  $1 - r$  credibility zone for the fragility curve:

$$\hat{\mathcal{S}}_L^{r|\mathbf{a}, \mathbf{z}} = \|\hat{q}_{1-r/2}^{\theta_{i=1}^L|\mathbf{a}, \mathbf{z}} - \hat{q}_{r/2}^{\theta_{i=1}^L|\mathbf{a}, \mathbf{z}}\|_{L^2}^2. \quad (17)$$

The  $L^2$  norms are integrals over  $a \in [0, A_{\max}]$  which are approximated numerically using Simpson's interpolation on a regular subdivision  $0 = A_0 < \dots < A_p = A_{\max}$ . In the forthcoming examples we use  $A_0 = 0$ ,  $A_{\max} = 12 \text{ m/s}^2$ ,  $p = 200$ .

For the MLE with bootstrapping, we can define a conditional quadratic error as in equation (16) and conditional width of the  $1 - r$  confidence interval as in equation (17) using a bootstrapped sample  $(\theta_i)_{i=1}^L$ .

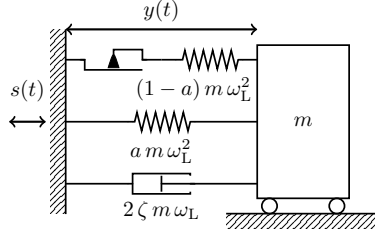


Figure 4: Elastoplastic oscillator with kinematic hardening, with parameters  $f_L = 5$  Hz and  $\zeta = 2\%$ . The yield limit is  $Y = 5 \cdot 10^{-3}$  m and the post-yield stiffness is 20% of the elastic stiffness, i.e.  $a = 0.2$ .

## 6. Numerical applications

In this section, three case studies are examined. The first is a nonlinear oscillator for which  $10^5$  nonlinear calculations have been implemented for validation purposes (section 6.1). The second case study corresponds to a piping system which is a part of a secondary line of a French Pressurized Water Reactor (section 6.2). In this case, only  $10^4$  calculations have been performed due to the high computational cost. Finally, the last case study concerns a stacked structure intended for the storage of packages (section 6.3). Only 21 test results performed on a shaking table are available for the fragility curve estimation in this case.

### 6.1. Case study 1: a nonlinear oscillator

#### 6.1.1. Description

This first case study - depicted in Figure 4 - relates to a single degree of freedom elastoplastic oscillator which exhibits kinematic hardening. This mechanical system reflects the essential features of the nonlinear responses of some real structures under seismic excitation and has already been used in several studies [24, 28, 34]. For a unit mass  $m$ , its equation of motion is:

$$\ddot{y}(t) + 2\zeta\omega_L\dot{y}(t) + f(t) = -s(t), \quad (18)$$

with  $s(t)$  a seismic signal.  $\dot{y}(t)$  and  $\ddot{y}(t)$  are respectively the relative velocity and acceleration of the mass.  $\zeta$  is the damping ratio and  $\omega_L$  is the circular frequency. The EDP of interest is the maximum in absolute value of the displacement of the mass, i.e.  $\max_{t \in [0, T]} |y(t)|$  where  $T$  is the duration of the seismic excitation. The failure criterion  $C$  is chosen to be the 90% quantile of the maximum displacement calculated with  $10^5$  artificial signals, i.e.  $C = 8.0 \cdot 10^{-3}$  m. Figure 5 shows the comparison between the reference MC-based fragility curve  $P_f^{MC}$  (equation (11)) and its log-normal estimate  $P_f^{MLE}$ , both estimated via the results of the  $10^5$  simulations. The log-normal fragility curve is here a good approximation of the reference curve.

#### 6.1.2. Results and discussion

Fragility curve estimates are shown in Figure 6. They result from  $L = 5000$  samples for  $\theta$  generated for each implemented method (section 5), for two samples of sizes  $k = 20$  and  $k = 30$ . Although the intervals compared - that of the Bayesian framework and that of the MLE - are not of the same nature - credibility interval for the first *versus* confidence interval for the second - these results clearly illustrate the advantage of the Bayesian framework over the MLE for small samples. Indeed, with the MLE appear irregularities characterized by null estimates of  $\beta$ , which result in "vertical" confidence intervals. When few failures are observed in the initial sample, some bootstrapped samples can be partitioned into two disjoint subsets when classified according to IM values: the one for which there is no failure and the one for which there is failure. As no prior is considered, the likelihood is therefore easily maximized with  $\beta = 0$ . In Appendix B, we prove that such scenarios result in degenerative likelihood. This last statement is perceived better through the inspection of the raw values of  $\theta$  generated in Figure 7. The degenerate  $\beta$  values that result from the MLE appear clearly and no such phenomenon is observed in the Bayesian framework. In Appendix B we present several possible scenarios which would cause such degeneracy within the Bayesian context.

Since the SK's prior is calibrated to look like the Jeffreys prior, Figure 6 shows a strong similarity between the Bayesian estimates of the fragility curves obtained with these two priors. However, Figure 7 (middle) shows that many

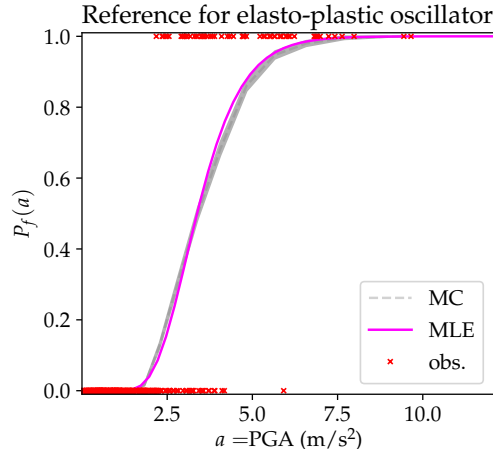


Figure 5: Reference fragility curve  $P_f^{MC}$  (see section 5.1) compared with  $P_f^{MLE}$  (see section 5.4) for the elastoplastic oscillator (case study 1). They are computed using the full data-set generated ( $10^5$  items). The red crosses represent the observations.

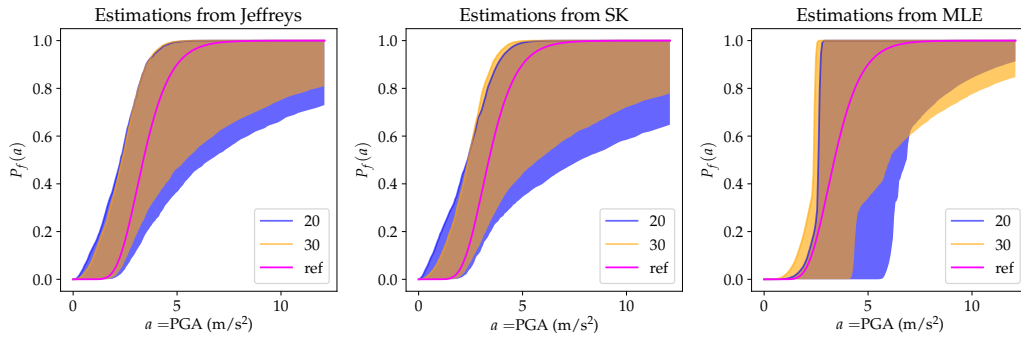


Figure 6: 95% credibility (for Bayesian estimation) or confidence (for MLE) intervals of fragility curves estimates, for the elastoplastic oscillator, resulting from a total of 5000 simulations of  $\theta$  using the three methods introduced in 5.3: (from left to right) Bayesian estimation using Jeffreys prior, Bayesian estimation using SK's prior, MLE with bootstrapping. For each of them, two data-samples of two different sizes are considered ( $k = 20$  in blue,  $k = 30$  in orange). In magenta is plotted  $P_f^{MLE}$ .

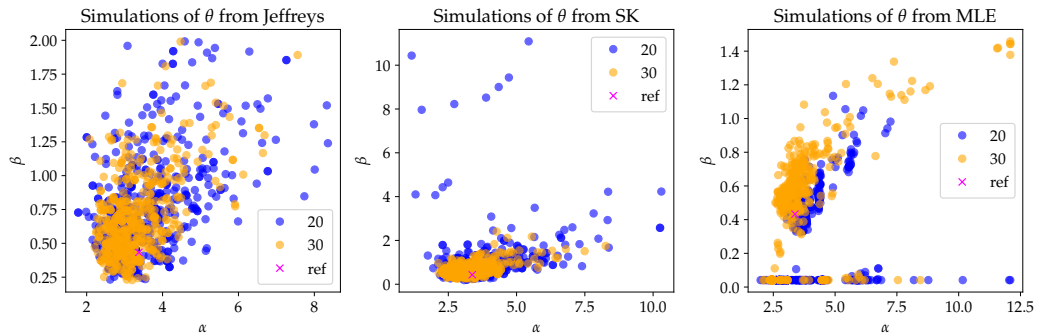


Figure 7: Scatter plots of the generated  $\theta$  to estimate the fragility curves presented in Figure 6 for the elasto-plastic oscillator. For the three methods and two data-sets (of size 20 in blue and 30 in orange) are plotted 500 points from the 5000  $\theta = (\alpha, \beta)$  generated. The magenta crosses stand for  $\theta^{MLE}$  which is used for the computation of  $P_f^{MLE}$ .

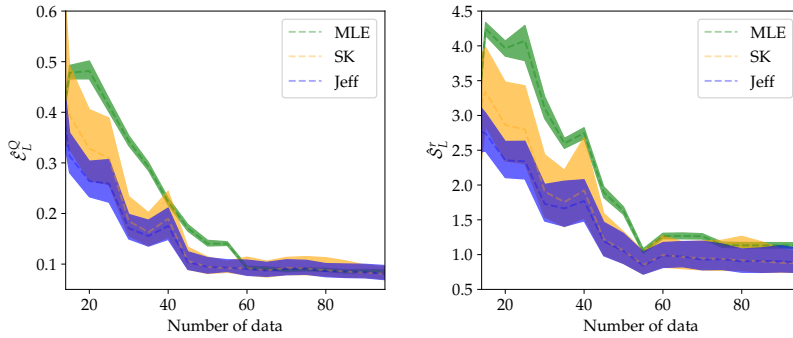


Figure 8: Performance evaluation metrics (see section 5.4) for the elasto-plastic oscillator computed by replications from independent draws in the total dataset and for sample sizes ranging from 15 to 100. Left: as a function of the number of observations, the dashed lines plot the quadratic errors and the shaded areas show their confidence intervals. Right: the dashed lines plot the widths of the credibility intervals (for Bayesian estimation) or confidence intervals (for MLE) and the shaded areas show their confidence intervals.

outliers are simulated with the SK’s prior. These values explain that the credibility intervals of the fragility curves are larger with the SK’s prior when  $k = 20$ . This observation is supported theoretically by the calculation we provide in Appendix B. Indeed, we have shown a better convergence of the Jeffreys prior toward 0 when  $\beta \rightarrow \infty$ . This better asymptotic behavior obviously results in posteriors which happen to give a lower probability to outlier points – phenomenon particularly noticeable when the data-sample is small – as well as to the weight of the likelihood within the posterior.

For a better understanding of this phenomenon, we calculate the quantitative metrics defined in section 5.4. For any  $k$  varying from 15 to 100,  $m = 200$  different draws of observations  $(\mathbf{a}^{(j)}, \mathbf{z}^{(j)})_{j=1}^m$  have been conducted to derive the metrics  $\hat{\mathcal{E}}_{L,R}^{Q|\mathbf{a}^{(j)}, \mathbf{z}^{(j)}}$ ,  $\hat{\mathcal{S}}_{L,R}^{r|\mathbf{a}^{(j)}, \mathbf{z}^{(j)}}$ ,  $j \in \{1, \dots, m\}$ ,  $R \in \{\text{‘MLE’}, \text{‘SK’}, \text{‘Jeffreys’}\}$ ,  $L = 5000$ ,  $1 - r = 95\%$ . Their means and their 95%-confidence intervals are plotted in Figure 8. First, these plots demonstrate the interest of the Bayesian framework compared to the MLE approach, with small observations sets. Second, the performance of the Jeffreys posterior in comparison with SK’s is highlighted by the confidence interval endpoints of the quadratic error and the credibility interval. The latter highlights the effect of the better asymptotic behavior of the Jeffreys prior on the width of the credibility interval, which varies similarly while being smaller than that of the SK prior, thus highlighting its ability to generate fewer outliers for the pair  $(\alpha, \beta)$  as expected.

## 6.2. Case study 2 : piping system

### 6.2.1. Description

This second case study concerns a piping system that is a part of a secondary line of a French Pressurized Water Reactor. This piping system was studied, experimentally and numerically, within the framework of the ASG program [53]. Figure 9 shows a view of the mock-up mounted on the shaking table Azalee of the EMSI laboratory of CEA/Saclay whereas the Finite Element Model (FEM) – based on beam elements – is shown in Figure 9-right. The latter has been implemented with the homemade FE code CAST3M [54] and has been validated via an experimental campaign.

The mock-up is a 114.3 mm outside diameter and 8.56 mm thickness pipe with a 0.47 elbow characteristic parameter, in carbon steel TU42C, filled with water without pressure. It has three elbows and a mass modeling a valve (120 kg) which corresponds to more than 30% of the total mass of the mock-up. One end of the mock-up is clamped whereas the other is supported by a guide in order to prevent the displacements in the X and Y directions. Additionally, a rod is placed on the top of the specimen to limit the mass displacements in the Z direction (see Figure 9-right). In the tests, the excitation is only imposed in the X direction. For this study, the artificial signals are filtered by a fictitious 2% damped linear single-mode building at 5 Hz, the first eigenfrequency of the 1% damped piping system. As failure criterion, we consider excessive out-of-plane rotation of the elbow located near the clamped end of the mock-up, as recommended in [55]. The critical rotation considered is equal to  $4.1^\circ$ . This is the level quantile 90% of a sample of numerical simulations of size  $10^4$ .

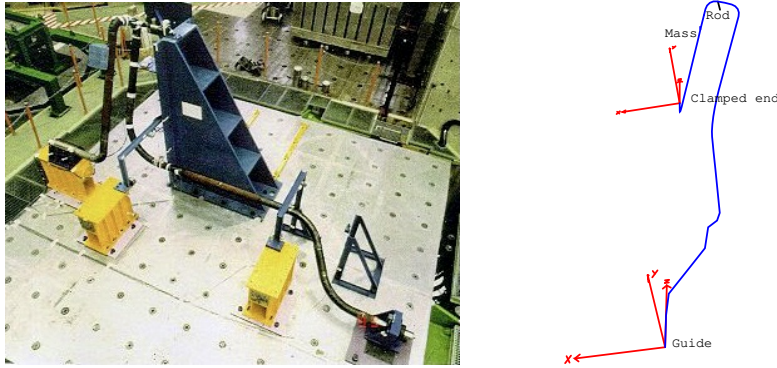


Figure 9: (left) Overview of the piping system on the Azalee shaking table and (right) Mock-up FEM

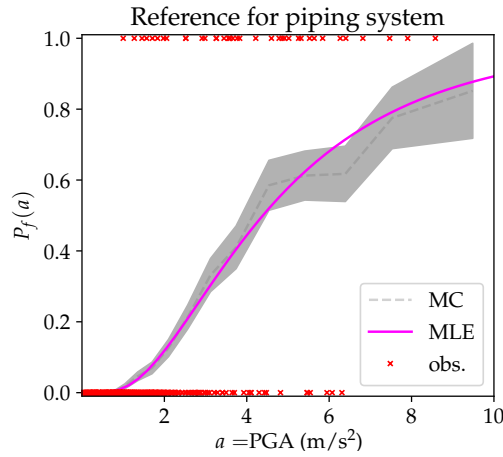


Figure 10: Reference fragility curve  $P_f^{MC}$  (see section 5.1) compared with  $P_f^{MLE}$  (see section 5.4) for the piping system (case study 2). They are computed using the full data-set generated ( $10^4$  items). The red crosses represent the observations.

Figure 10 shows the comparison between the reference MC-based fragility curve  $P_f^{MC}$  (equation (11)) and its log-normal estimate  $P_f^{MLE}$ , both estimated via the results of  $10^4$  simulations. The log-normal fragility curve is also here a good approximation of the reference curve.

### 6.2.2. Results and discussion

Similar simulations to those carried out for the elastoplastic oscillator have been performed for this case study and they highlight the same trends. Indeed, for sets of 5000 values of  $\theta$  – generated with each method considered in this work – and for two sample sizes  $k = 20$  and  $k = 30$ , Figure 11 shows as expected the superiority of the Bayesian framework over the coupled MLE and bootstrap approach. As in the case of the oscillator, we see the same irregularities with the MLE-based approach: the confidence intervals are ”quasi-vertical”, reflecting many estimates of  $\beta$  equal to 0. Moreover, the credibility intervals are wider with the SK’s prior than with Jeffreys prior, reflecting here also more outliers of  $\theta$  generated with the SK’s prior. These observations are clearly supported by the results presented in Figure 12.

For a more complete overview of their relative performance, the evaluation metrics described in section 5.4 have been computed in the same way as for the first case study:  $m = 200$  draws of data samples  $(\mathbf{a}^{(j)}, \mathbf{z}^{(j)})_{j=1}^m$  have been randomly chosen to compute, for any value of  $k$  varying in a range from 15 to 100,  $m$  values of the metrics  $\hat{\mathcal{E}}_{L,R}^{Q|\mathbf{a}^{(j)}, \mathbf{z}^{(j)}}$ ,

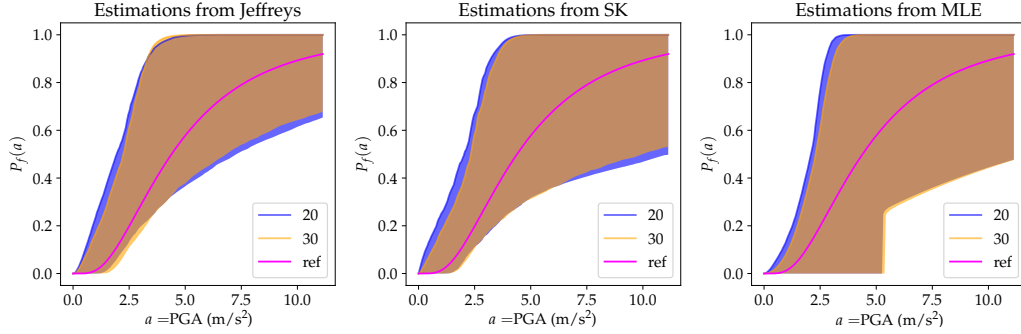


Figure 11: 95% credibility (for Bayesian estimation) or confidence (for MLE) intervals of fragility curves estimates, for the piping system, resulting from a total of 5000 simulations of  $\theta$  using the three methods introduced in 5.3: (from left to right) Bayesian estimation using Jeffreys prior, using SK's prior, MLE with bootstrapping. For each of them, two data samples of two different sizes are considered ( $k = 20$  in blue,  $k = 30$  in orange). In magenta is plotted  $P_f^{\text{MLE}}$ .

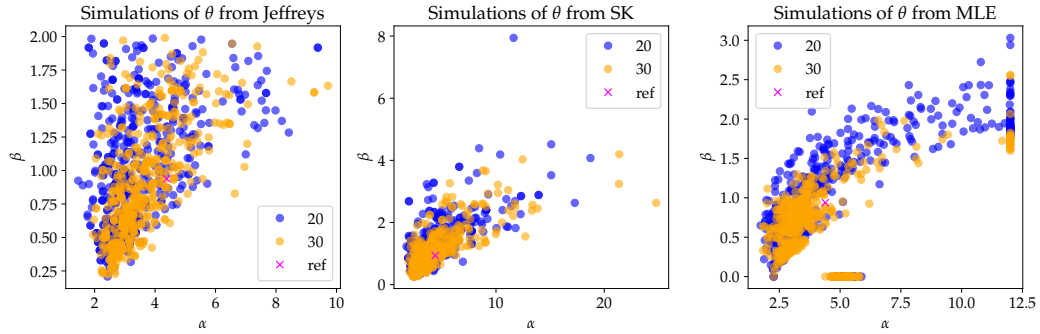


Figure 12: Scatter plots of the generated  $\theta$  to estimate the fragility curves presented in Figure 11 for the piping system. For the three methods and two data-sets (of size 20 in blue and 30 in orange) are plotted 500 points from the 5000  $\theta = (\alpha, \beta)$  generated. The magenta crosses plot  $\theta^{\text{MLE}}$  which is used for the computation of  $P_f^{\text{MLE}}$ .

$\hat{S}_{L,R}^{\text{ref}(\theta, \mathbf{x}^{(j)})}$ ,  $R \in \{\text{'MLE'}, \text{'SK'}, \text{'Jeffreys'}\}$ ,  $L = 5000$ ,  $1 - r = 95\%$ . Their means and confidence intervals are proposed in Figure 13. These results confirm the better performance of the Jeffreys prior compared to the other two methods.

### 6.3. Case study 3 : free-standing stacked structure

#### 6.3.1. Description

The last case study concerns a free-standing stacked structure composed of three pallets intended for the storage of packages. As shown in Figure 14, it is a square-based structure 3 meters high with a slenderness of 2.4.

The mass of one package is equal to 265 kg whereas the mass of one pallet is equal to 60 kg. The total mass of the structure is equal to 3 360 kg. The pallets are made of 3 mm thick hollow section aluminum square tubes. These tubes are welded and form the base and uprights of the pallets. The base of a pallet supports four free-standing packages whereas the uprights support the upper free-standing pallet(s). The stacked structure was studied in [56] by means, among others, of a complete experimental campaign which was carried out on a 1D shaking table of CEA/Saclay. In particular, the stack was subjected to 21 of the 97 real signals that were used for database enrichment in [28]. For this structure, the failure criterion relates to excessive displacement of the top of the stack. An example of a test result is shown in Figure 14 which depicts the horizontal displacements over time of the top of the stack. The initial position is indicated in red while the different positions in time are in blue. Due to uplift, sliding and rotation motions, the top of the stack exceeds, for this test, the admissibility criterion which is materialized in black. This criterion was chosen to be the 90% level quantile of the 21 test results. Due to the signals used for these tests, the Jeffreys prior is suitable for

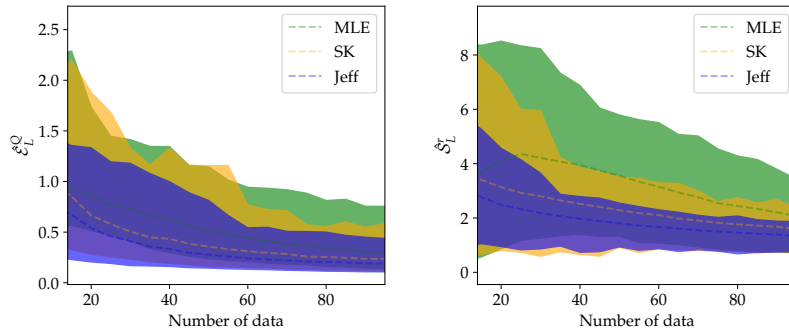


Figure 13: Performance evaluation metrics (see section 5.4) for the piping system computed by replications from independent draws in the total data set and for sample sizes ranging from 15 to 100. Left: as a function of the number of observations, the dashed lines plot the quadratic errors and the shaded areas show their confidence intervals. Right: the dashed lines plot the widths of the credibility intervals (for Bayesian estimation) or confidence intervals (for MLE) and the shaded areas show their confidence intervals.

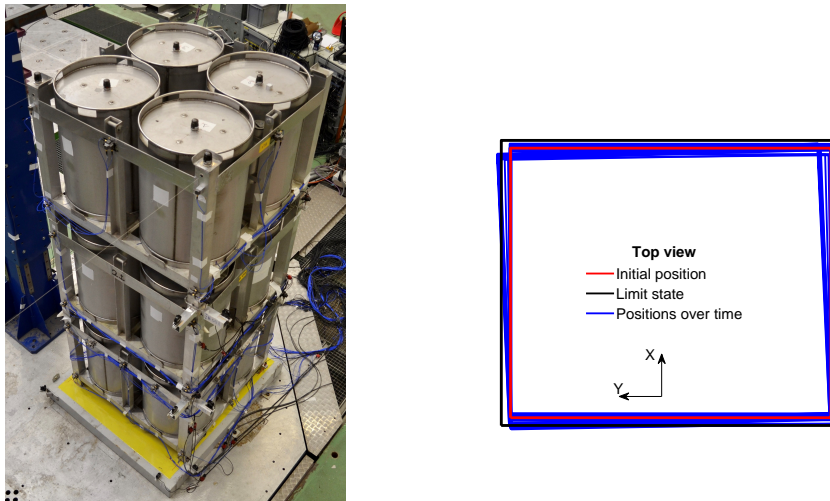


Figure 14: (left) Overview of the stacked structure placed on the Vesuve 1D shaking table and (right) example of test result: horizontal displacements of the top of the stack when subjected to seismic excitation in the X direction.

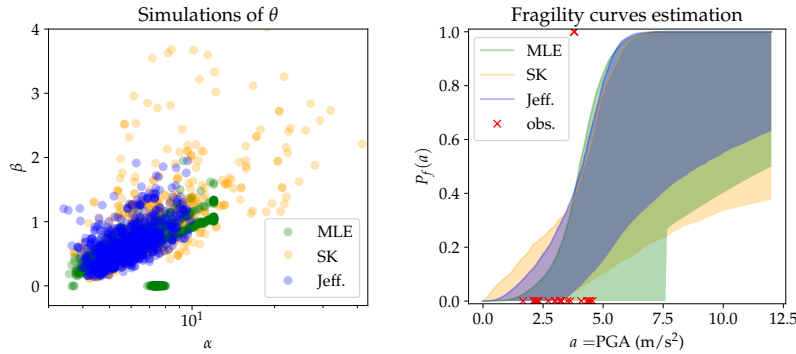


Figure 15: Estimations results for the stacked structure. Each of the three methods introduced in section 5.3 led to 5000 points generated (left figure, with  $\alpha$  in log scale). On the right are exposed the three 95% credibility (for Bayesian estimation) or confidence (for MLE) intervals that result. The red crosses represent the 21 test results.

estimating the fragility curve of the stack from the 21 test results. The SK’s prior calibrated to approximate Jeffreys’ prior can also be used.

### 6.3.2. Results and discussion

The small number of data does not allow comparison with a reference. Therefore, only a qualitative study can be carried out. Figure 15 shows the results from 5000 estimations of  $\theta$  performed with the three methods. These results do not call into question the previous ones because they, once again, highlight the same phenomena, namely: (i) some irregularities of the MLE-based approach characterized by “quasi-vertical” confidence intervals, (ii) wider credibility intervals with the SK’s prior than with Jeffreys prior and (iii) the generation of a large number of outliers of  $\theta$  with SK’s posterior compared to Jeffreys posterior, which explains the slightly larger credibility intervals on the log-normal estimates of the fragility curves.

## 7. Conclusion

Assessing the seismic fragility of Structures and Components when little data is available is a daunting task. The Bayesian framework is known to be efficient for this kind of problems. Nevertheless, the choice of the prior remains tricky because it has a non-negligible influence on the *a posteriori* distribution and therefore on the estimation of any quantity of interest linked to the fragility curves.

So, based on the reference prior theory to define an objective prior, we have derived the Jeffreys prior for the log-normal model with binary data which indicate the state of the structure (e.g. failure or non-failure). In doing so, this prior is completely defined, it does not depend on an additional subjective choice.

In comparison with the classic approaches proposed in the literature, we show rigorously – i.e. both theoretically and numerically – the robustness and advantages of the proposed approach in terms of regularization (absence of degenerate estimation) and stability (absence of outliers when sampling the *a posteriori* distribution of the parameters) for fragility curves estimation.

Although its numerical implementation is complex — i.e. more complex than a prior defined as the product of two classical distributions such as log-normal distributions for instance – it is not a major obstacle. In fact, depending solely on the distribution of the IM, its initial calculation will be quickly valued on the scale of an industrial installation which includes several SCs whose fragility curves must be evaluated.

## 8. Acknowledgments

This research was supported by CEA (French Alternative Energies and Atomic Energy Commission) and SEISM Institute ([www.institut-seism.fr/en/](http://www.institut-seism.fr/en/)).

## Appendix A. Calculation of the Fisher information matrix

In this section we compute the Fisher information matrix that gives the expression of the Jeffreys prior. Denoting  $\gamma = \gamma(a) = \beta^{-1} \log \frac{a}{\alpha}$ , the first-order partial derivatives with respect to  $\theta$  of  $\log p(z|a, \theta)$  are:

$$\frac{\partial}{\partial \alpha} \log p(z|a, \theta) = -\frac{1}{\alpha\beta} z \frac{\Phi'(\gamma)}{\Phi(\gamma)} + \frac{1}{\alpha\beta} (1-z) \frac{\Phi'(\gamma)}{1-\Phi(\gamma)}, \quad (\text{A.1})$$

$$\frac{\partial}{\partial \beta} \log p(z|a, \theta) = -\frac{\log \frac{a}{\alpha}}{\beta^2} z \frac{\Phi'(\gamma)}{\Phi(\gamma)} + \frac{\log \frac{a}{\alpha}}{\beta^2} (1-z) \frac{\Phi'(\gamma)}{1-\Phi(\gamma)}, \quad (\text{A.2})$$

and the second-order partial derivatives are:

$$\begin{aligned} \frac{\partial^2}{\partial \alpha \partial \beta} \log p(z|a, \theta) &= -\frac{1}{\beta} \frac{\partial}{\partial \alpha} \log p(z|a, \theta) + \frac{\log \frac{a}{\alpha}}{\alpha\beta^3} z \frac{\Phi''(\gamma)\Phi(\gamma) - \Phi'(\gamma)^2}{\Phi(\gamma)^2} \\ &\quad - \frac{\log \frac{a}{\alpha}}{\alpha\beta^3} (1-z) \frac{\Phi''(\gamma)(1-\Phi(\gamma)) + \Phi'(\gamma)^2}{(1-\Phi(\gamma))^2}, \end{aligned} \quad (\text{A.3})$$

$$\begin{aligned} \frac{\partial^2}{\partial \alpha^2} \log p(z|a, \theta) &= -\frac{1}{\alpha} \frac{\partial}{\partial \alpha} \log p(z|a, \theta) + \frac{1}{\alpha^2\beta^2} z \frac{\Phi''(\gamma)\Phi(\gamma) - \Phi'(\gamma)^2}{\Phi(\gamma)^2} \\ &\quad - \frac{1}{\alpha^2\beta^2} (1-z) \frac{\Phi''(\gamma)(1-\Phi(\gamma)) + \Phi'(\gamma)^2}{(1-\Phi(\gamma))^2}, \end{aligned} \quad (\text{A.4})$$

and

$$\begin{aligned} \frac{\partial^2}{\partial \beta^2} \log p(z|a, \theta) &= -\frac{2}{\beta} \frac{\partial}{\partial \beta} \log p(z|a, \theta) + \frac{\log^2 \frac{a}{\alpha}}{\beta^4} z \frac{\Phi''(\gamma)\Phi(\gamma) - \Phi'(\gamma)^2}{\Phi(\gamma)^2} \\ &\quad - \frac{\log^2 \frac{a}{\alpha}}{\beta^4} (1-z) \frac{\Phi''(\gamma)(1-\Phi(\gamma)) + \Phi'(\gamma)^2}{(1-\Phi(\gamma))^2}. \end{aligned} \quad (\text{A.5})$$

The expressions of the second-order partial derivatives of  $p(z|a, \theta)$  derived in equations (A.3), (A.4) and (A.5) need to be integrated over  $\mathcal{Z}$  and  $\mathcal{A}$ . Integrating over the discrete variable  $z$  first replaces  $z$  by  $\Phi(\gamma)$  and  $(1-z)$  by  $1-\Phi(\gamma)$  in the equations. Finally, if we denote

$$\begin{aligned} A_{01} &= \int_{\mathcal{A}} \frac{\Phi'(\gamma(a))^2}{\Phi(\gamma(a))} p(a) da, & A_{02} &= \int_{\mathcal{A}} \frac{\Phi'(\gamma(a))^2}{\Phi(-\gamma(a))} p(a) da, \\ A_{11} &= \int_{\mathcal{A}} \log \frac{a}{\alpha} \frac{\Phi'(\gamma(a))^2}{\Phi(\gamma(a))} p(a) da, & A_{12} &= \int_{\mathcal{A}} \log \frac{a}{\alpha} \frac{\Phi'(\gamma(a))^2}{\Phi(-\gamma(a))} p(a) da, \\ A_{21} &= \int_{\mathcal{A}} \log^2 \frac{a}{\alpha} \frac{\Phi'(\gamma(a))^2}{\Phi(\gamma(a))} p(a) da, & A_{22} &= \int_{\mathcal{A}} \log^2 \frac{a}{\alpha} \frac{\Phi'(\gamma(a))^2}{\Phi(-\gamma(a))} p(a) da, \end{aligned} \quad (\text{A.6})$$

then the information matrix  $\mathcal{I}(\theta)$  has the following form

$$\mathcal{I}(\theta) = \begin{pmatrix} \frac{1}{\alpha^2\beta^2} (A_{01} + A_{02}) & \frac{1}{\alpha\beta^3} (A_{11} + A_{12}) \\ \frac{1}{\alpha\beta^3} (A_{11} + A_{12}) & \frac{1}{\beta^4} (A_{21} + A_{22}) \end{pmatrix}. \quad (\text{A.7})$$

Integration with respect to  $a$  is proceeded using Simpson's interpolation on a regular grid  $A_0 < \dots < A_p$ ,  $A_0 = 0$ ,  $A_p = 12 \text{ m/s}^2$ ,  $p = 200$ . The distribution  $p(a)$  is approximated from the  $10^5$  PGA derived from the generated seismic signals discussed in section 4.2. This approximation is expressed as a sum of Gaussian kernels.

## Appendix B. Prior and posterior asymptotics

This section is dedicated to the asymptotic study of the density functions that are considered in this work. Those calculations provide a proof of the proper characteristics of the posterior distributions, needed to validate MCMC methods for sampling the posterior distributions. Also, the asymptotics of Jeffreys prior can be compared to the ones of [Straub and Der Kiureghian](#)'s prior to state rigorously their different convergence rates.

The analysis of Jeffreys prior convergence rates requires an assumption about the IM's distribution. Here we consider the following one.

**Assumption 1.** The IM is distributed according to a log-normal distribution. i.e. there exist  $\mu, \sigma$  such that

$$p(a) = \frac{1}{\sqrt{2\pi\sigma^2 a}} \exp\left(-\frac{(\log a - \mu)^2}{2\sigma^2}\right). \quad (\text{B.1})$$

This assumption, not far from reality, meets the discussion we conducted in section 5.3.2. It makes SK's prior being given by

$$\pi_{SK}(\theta) = \frac{1}{\sqrt{2\pi\sigma^2 \alpha\beta}} \exp\left(-\frac{(\log \alpha - \mu)^2}{2\sigma^2}\right). \quad (\text{B.2})$$

The following is organized as follows: [Appendix B.1](#) summarizes and discusses our theoretical results. The proofs are then presented in [Appendix B.2](#).

### Appendix B.1. Results

The following proposition gives the asymptotic behaviors of the likelihood in several directions.

**Proposition 1.** Consider  $k > 1$  and a data sample  $(\mathbf{a}, \mathbf{z}) = ((a_i)_{i=1}^k, (z_i)_{i=1}^k)$ . Introduce the vectors  $\mathbf{N} = (z_i \mathbb{1}_{a_i < \alpha} + (1 - z_i) \mathbb{1}_{a_i > \alpha})_{i=1}^k$ ,  $\log^2 \frac{\mathbf{a}}{\alpha} = (\log^2 \frac{a_i}{\alpha})_{i=1}^k$ .

- Fix  $\alpha > 0$ , then

$$\ell_k(\mathbf{z}|\mathbf{a}, \theta) \xrightarrow{\beta \rightarrow \infty} 2^{-k} \quad (\text{B.3})$$

and

$$\ell_k(\mathbf{z}|\mathbf{a}, \theta) \underset{\beta \rightarrow 0}{=} O\left(\beta^{|\mathbf{N}|} e^{-\frac{\mathbf{N}^T \log^2 \frac{\mathbf{a}}{\alpha}}{2\beta^2}}\right), \quad (\text{B.4})$$

where  $|\mathbf{N}| = \sum_{i=1}^k N_i$ .

- Fix  $\beta > 0$ , then

$$\ell_k(\mathbf{z}|\mathbf{a}, \theta) \underset{\alpha \rightarrow 0}{=} O\left(|\log \alpha|^{|\mathbf{z}|-k} e^{-\frac{1}{2\beta^2} \sum_{i=1}^k (1-z_i)(\log a_i - \log \alpha)^2}\right) \quad (\text{B.5})$$

and

$$\ell_k(\mathbf{z}|\mathbf{a}, \theta) \underset{\alpha \rightarrow \infty}{=} O\left(\log(\alpha)^{-|\mathbf{z}|} e^{-\frac{1}{2\beta^2} \sum_{i=1}^k z_i (\log a_i - \log \alpha)^2}\right), \quad (\text{B.6})$$

where  $|\mathbf{z}| = \sum_{i=1}^k z_i$  is the number of failures in the observed sample.

The high rate of convergence to 0 of the likelihood when  $\beta \rightarrow 0$  stated above is not ensured under a few circumstances. In fact, if the failure occurrences are perfectly separated (i.e. there exists an open interval  $U$  such that  $\forall \alpha \in U, \forall i, z_i = 1 \iff a_i > \alpha$ ), then the vector  $\mathbf{N}$  is equal to  $\mathbf{0}$  for any  $\alpha \in U$ . For  $\alpha$  in this interval, the likelihood does not converge to zero when  $\beta \rightarrow 0$ . Also, the convergence of the likelihood to zero is not established if the observed sample only contains one type of scenario (among failures and no-failures).

The next three propositions give the asymptotics of the Jeffreys prior  $J(\theta)$  for  $\theta = (\alpha, \beta)$  in the four main directions of  $(0, +\infty)^2$ .

**Proposition 2.** Fix  $\alpha > 0$ , there exists  $D'(\alpha) > 0$  such that

$$J(\theta) \underset{\beta \rightarrow 0}{\sim} \frac{D'(\alpha)}{\beta}. \quad (\text{B.7})$$

**Proposition 3.** Fix  $\alpha > 0$ , there exists a constant  $E' > 0$  such that

$$J(\theta) \underset{\beta \rightarrow \infty}{\sim} \frac{E'}{\alpha \beta^3}. \quad (\text{B.8})$$

**Proposition 4.** Fix  $\beta > 0$ , there exists  $G''(\beta) > 0$  such that

$$J(\theta) \underset{|\log \alpha| \rightarrow \infty}{\sim} G''(\beta) \frac{|\log \alpha|}{\alpha} \exp\left(-\frac{(\log \alpha - \mu)^2}{2\beta^2 + 2\sigma^2}\right). \quad (\text{B.9})$$

*Proper characteristic discussion.* Those results confirm that Jeffreys and SK's priors are not proper with respect to  $\beta$ . For Jeffreys prior, its divergence and convergence rates with respect to  $\beta$  make its resulting posterior being proper when the prior is coupled with the likelihood. However, one can see that this is not the case for SK's posterior, which is not integrable w.r.t.  $\beta$ , because of its too low convergence rate at  $+\infty$ . This makes the MCMC simulations from this posterior impossible to validate, unless considering a truncation of the distribution. This statement explains the generation of a posteriori outliers using SK's prior. Note that [Straub and Der Kiureghian](#) consider this prior within a Bayesian framework in [14] which is slightly different from ours. In [Appendix C](#) we confirm that the posterior is not proper even when derived in the exact framework of [14].

*Jeffreys and SK's priors asymptotic comparison.* By comparing Jeffreys prior asymptotics with SK's prior asymptotics (B.2), we can notice the following:

- Regarding their asymptotics w.r.t.  $\beta$ , while their divergence rates are the same when  $\beta \rightarrow 0$ , Jeffreys prior performs better when  $\beta \rightarrow \infty$ :

$$J(\theta) \propto \beta^{-2} \pi_{SK}(\theta).$$

Consequently, SK's posterior gives higher probabilities to high values of  $\beta$  compared to Jeffreys prior.

- Regarding their asymptotics w.r.t.  $\alpha$ , both are asymptotically close to a log-normal distribution, with a disadvantage on the side of Jeffreys prior, for which the asymptotic variance is derived by adding  $\beta^2$  to the one of SK's prior. Thus, while for small values of  $\beta$  (smaller than  $\sigma$ ) both priors remain comparable w.r.t.  $\alpha$ , Jeffreys prior gives higher probabilities to outliers  $\alpha$  when  $\beta$  is high itself. However, as seen above large values of  $\beta$  have a quite low probability in the case of Jeffreys prior compared with SK prior. This explains why the generation of such outliers  $\alpha$  has not been encountered in the simulations performed in our paper.

## Appendix B.2. Proofs

We first state some upper bounds for the function  $\gamma \mapsto [\Phi(\gamma)(1 - \Phi(\gamma))]^{-1}$ . The following lemmas are proven below.

**Lemma 1.** For any  $\gamma \in \mathbb{R}$ ,  $[\Phi(\gamma)(1 - \Phi(\gamma))]^{-1} \leq 4 \exp(2\gamma^2/\pi)$ .

**Lemma 2.** For any  $\gamma \in \mathbb{R}$ ,

$$\Phi(\gamma)(1 - \Phi(\gamma)) \geq \frac{\sqrt{2/\pi} \exp(-\gamma^2/2)}{(|\gamma| + \sqrt{\gamma^2 + 4})}. \quad (\text{B.10})$$

*Proof of lemma 1.* We remind the following inequality about the erf function [57]:

$$\forall \gamma > 0, \sqrt{1 - e^{-\frac{\gamma^2}{2}}} \leq \text{erf}(\gamma/\sqrt{2}) \leq \sqrt{1 - e^{-2\frac{\gamma^2}{\pi}}}.$$

Fix  $\gamma > 0$  and deduce

$$\begin{aligned} e^{-\frac{2\gamma^2}{\pi}} &\leq 1 - \text{erf}(\gamma/\sqrt{2})^2 \leq e^{-\frac{\gamma^2}{2}}, \\ \frac{1}{4} e^{-\frac{2\gamma^2}{\pi}} &\leq \frac{1}{4} (1 - \text{erf}(\gamma/\sqrt{2})) (1 + \text{erf}(\gamma/\sqrt{2})) \leq \frac{1}{4} e^{-\frac{\gamma^2}{2}}, \end{aligned}$$

the middle hand term being equal to  $\Phi(\gamma)(1 - \Phi(\gamma))$ , which implies when applying the inverse:

$$[\Phi(\gamma)(1 - \Phi(\gamma))]^{-1} \leq 4e^{\frac{2\gamma^2}{\pi}},$$

hence the result for  $\gamma > 0$ .

While it is clear that the inequality still stands for  $\gamma = 0$ , notice from  $\Phi(-\gamma) = 1 - \Phi(\gamma) \forall \gamma \in \mathbb{R}$  that  $\gamma \mapsto \Phi(\gamma)(1 - \Phi(\gamma))$  is an even function. Thus, the inequality still stands for any  $\gamma < 0$ ; this concludes the proof of the lemma.  $\square$

*Proof of lemma 2.* Komatsu's inequality [58, p. 17]:

$$\forall \gamma > 0, \frac{2}{\sqrt{\gamma^2 + 4 + \gamma}} \leq e^{\frac{\gamma^2}{2}} \int_{\gamma}^{\infty} e^{-\frac{t^2}{2}} dt \leq \frac{2}{\sqrt{\gamma^2 + 2 + \gamma}}$$

implies

$$\forall \gamma > 0, \frac{2e^{-\frac{\gamma^2}{2}}}{\sqrt{\gamma^2 + 4 + \gamma}} \leq \sqrt{2\pi}(1 - \Phi(\gamma)) \leq \frac{2e^{-\frac{\gamma^2}{2}}}{\sqrt{\gamma^2 + 2 + \gamma}}$$

as  $0 < \Phi < 1$  it comes for  $\gamma > 0$

$$\Phi(\gamma)(1 - \Phi(\gamma)) \geq \frac{2e^{-\frac{\gamma^2}{2}}}{\sqrt{\gamma^2 + 4 + \gamma}} \left(1 - \frac{2e^{-\frac{\gamma^2}{2}}}{\sqrt{\gamma^2 + 2 + \gamma}}\right) \geq \frac{\sqrt{2/\pi}e^{-\frac{\gamma^2}{2}}}{\sqrt{\gamma^2 + 4 + \gamma}}.$$

Finally, as  $\Phi(-\gamma) = 1 - \Phi(\gamma)$ ,  $\gamma \mapsto \Phi(\gamma)(1 - \Phi(\gamma))$  is an even function and we have for any  $\gamma \in \mathbb{R}$

$$\Phi(\gamma)(1 - \Phi(\gamma)) \geq \frac{\sqrt{2/\pi}e^{-\frac{\gamma^2}{2}}}{\sqrt{\gamma^2 + 4 + |\gamma|}}.$$

$\square$

### Appendix B.2.1. Proof of Proposition 1

We recall the likelihood expression:

$$\begin{aligned} \ell_k(\mathbf{z}, \mathbf{a}, \theta) &= \prod_{i=1}^k \Phi\left(\frac{\log a_i - \log \alpha}{\beta}\right)^{z_i} \left(1 - \Phi\left(\frac{\log a_i - \log \alpha}{\beta}\right)\right)^{1-z_i} \\ &= \exp\left[\sum_{i=1}^k (z_i \log \Phi(\gamma_i) + (1 - z_i) \log(1 - \Phi(\gamma_i)))\right], \end{aligned}$$

denoting  $\gamma_i = \beta^{-1} \log \frac{a_i}{\alpha}$ .

To treat the case  $\beta \rightarrow \infty$  we remark that while  $\alpha$  is fixed, the quantities  $\Phi(\gamma_i)$  will all converge to  $1/2$ . The product of those limits gives the limit  $\ell_k(\mathbf{z}|\mathbf{a}, \theta) \xrightarrow{\beta \rightarrow \infty} 2^{-k}$ .

For the other cases, we remind that  $\Phi(x) = \frac{1}{2}(1 + \operatorname{erf}(x/\sqrt{2}))$  and  $\operatorname{erf}(x) \underset{x \rightarrow \infty}{=} 1 - \frac{e^{-x^2}}{x\sqrt{\pi}} + o\left(\frac{e^{-x^2}}{x}\right)$ , leading to

$$\Phi(x) \underset{x \rightarrow \infty}{=} 1 - \frac{e^{-\frac{x^2}{2}}}{x\sqrt{2\pi}} + o\left(\frac{e^{-\frac{x^2}{2}}}{x}\right). \quad (\text{B.11})$$

Consider an  $i \in \{1, \dots, k\}$  and compute

$$\begin{aligned}
& z_i \log \Phi(\gamma_i) + (1 - z_i) \log(1 - \Phi(\gamma_i)) \\
& \stackrel{\gamma_i \rightarrow \infty}{=} z_i \log \left( 1 - \frac{e^{-\frac{\gamma_i^2}{2}}}{\gamma_i \sqrt{2\pi}} + o\left(\frac{e^{-\frac{\gamma_i^2}{2}}}{\gamma_i}\right) \right) + (1 - z_i) \log \left( \frac{e^{-\frac{\gamma_i^2}{2}}}{\gamma_i \sqrt{2\pi}} + o\left(\frac{e^{-\frac{\gamma_i^2}{2}}}{\gamma_i}\right) \right) \\
& \stackrel{\gamma_i \rightarrow \infty}{=} -z_i \frac{e^{-\frac{\gamma_i^2}{2}}}{\gamma_i \sqrt{2\pi}} + (1 - z_i) \log \left( \frac{e^{-\frac{\gamma_i^2}{2}}}{\gamma_i \sqrt{2\pi}} \right) + o(1) \\
& \stackrel{\gamma_i \rightarrow \infty}{=} -(1 - z_i) \frac{\gamma_i^2}{2} - (1 - z_i) \log(\gamma_i \sqrt{2\pi}) + o(1).
\end{aligned}$$

Using the relation  $\Phi(-x) = 1 - \Phi(x)$  leads to

$$z_i \log \Phi(\gamma_i) + (1 - z_i) \log(1 - \Phi(\gamma_i)) \stackrel{\gamma_i \rightarrow -\infty}{=} -z_i \frac{\gamma_i^2}{2} - z_i \log(-\gamma_i \sqrt{2\pi}) + o(1).$$

Going back to the likelihood asymptotics, we firstly fix  $\alpha > 0$  and suppose  $\beta \rightarrow 0$ . Thus, denoting the vectors  $\mathbf{N} = (z_i \mathbb{1}_{a_i < \alpha} + (1 - z_i) \mathbb{1}_{a_i > \alpha})_{i=1}^k$  and  $\log^2 \frac{\mathbf{a}}{\alpha} = (\log^2 \frac{a_i}{\alpha})_{i=1}^k$ , we obtain

$$\ell_k(\mathbf{z}|\mathbf{a}, \theta) \stackrel{\beta \rightarrow 0}{=} \frac{C(\alpha)}{\sqrt{2\pi}^{|\mathbf{N}|}} \beta^{|\mathbf{N}|} e^{-\frac{\mathbf{N}^T \log^2 \frac{\mathbf{a}}{\alpha} + o(1)}{2\beta^2}} \stackrel{\beta \rightarrow 0}{=} O\left(\beta^{|\mathbf{N}|} e^{-\frac{\mathbf{N}^T \log^2 \frac{\mathbf{a}}{\alpha}}{2\beta^2}}\right),$$

where  $|\mathbf{N}| = \sum_{i=1}^k N_i$  and  $C(\alpha) = \prod_{i=1}^k \left| \log \frac{a_i}{\alpha} \right|^{N_i}$ .

Secondly, fix  $\beta > 0$  to get

$$\begin{aligned}
\ell_k(\mathbf{z}|\mathbf{a}, \theta) & \stackrel{\alpha \rightarrow \infty}{=} \frac{\beta^{|\mathbf{N}|}}{\sqrt{2\pi}^{|\mathbf{N}|}} \left( \prod_{i=1}^k \log \left( \frac{\alpha}{a_i} \right)^{-z_i} \right) e^{-\frac{1}{2\beta^2} \sum_{i=1}^k z_i (\log a_i - \log \alpha)^2 + o(1)} \\
& \stackrel{\alpha \rightarrow \infty}{=} O\left(\log(\alpha)^{-|\mathbf{z}|} e^{-\frac{1}{2\beta^2} \sum_{i=1}^k z_i (\log a_i - \log \alpha)^2}\right),
\end{aligned}$$

where  $|\mathbf{z}| = \sum_{i=1}^k z_i$  is the number of failures in the observed sample. In the same way we have

$$\begin{aligned}
\ell_k(\mathbf{z}|\mathbf{a}, \theta) & \stackrel{\alpha \rightarrow 0}{=} \frac{\beta^{|\mathbf{N}|}}{\sqrt{2\pi}^{|\mathbf{N}|}} \left( \prod_{i=1}^k \log \left( \frac{a_i}{\alpha} \right)^{-(1-z_i)} \right) e^{-\frac{1}{2\beta^2} \sum_{i=1}^k (1-z_i) (\log a_i - \log \alpha)^2 + o(1)} \\
& \stackrel{\alpha \rightarrow 0}{=} O\left(|\log \alpha|^{|\mathbf{z}|-k} e^{-\frac{1}{2\beta^2} \sum_{i=1}^k (1-z_i) (\log a_i - \log \alpha)^2}\right).
\end{aligned}$$

### Appendix B.2.2. Proof of proposition 2

Let  $\alpha > 0$ . For  $0 \leq k \leq 2$ , we consider  $A_{k1,k2} = A_{k1} + A_{k2}$  with  $A_{kj}$  defined in (A.6):

$$A_{k1,k2} = \int_0^\infty \log^k \frac{a}{\alpha} \frac{\Phi'(\gamma(a))^2}{\Phi(\gamma(a))(1 - \Phi(\gamma(a)))} p(a) da.$$

We have

$$A_{k1,k2} = \beta^{k+1} \int_{-\infty}^\infty F_{A_{k1,k2}}(\gamma) d\gamma, \tag{B.12}$$

$$F_{A_{k1,k2}}(\gamma) = \frac{\gamma^k}{2\sqrt{\pi^3}\sigma^2} \frac{e^{-\gamma^2} e^{-\frac{(\beta\gamma - \mu + \log \alpha)^2}{2\sigma^2}}}{\Phi(\gamma)(1 - \Phi(\gamma))}. \tag{B.13}$$

By lemma 1 and upper bound can be derived for  $F_{A_{k1,k2}}$ : for any  $\gamma \in \mathbb{R}$ ,  $\beta > 0$ ,

$$|F_{A_{k1,k2}}(\gamma)| \leq \tilde{C}|\gamma|^k e^{-\frac{1}{3}\gamma^2} \quad (\text{B.14})$$

which defines an integrable function on  $\mathbb{R}$ ,  $\tilde{C}$  being a constant of  $\gamma$  and  $\beta$ . Hence the limit

$$\lim_{\beta \rightarrow 0} \int_{-\infty}^{\infty} F_{A_{k1,k2}}(\gamma) d\gamma = \int_{-\infty}^{\infty} \frac{\gamma^k}{2\sqrt{\pi^3\sigma^2}} \frac{e^{-\gamma^2} e^{-\frac{(\mu-\log \alpha)^2}{2\sigma^2}}}{\Phi(\gamma)(1-\Phi(\gamma))} d\gamma.$$

The last integral is null when  $k = 1$  as the integrated function is odd in this case. Otherwise, it is the integral of positive-valued function a.e. and so it is a positive constant. This way, we can state  $A_{k1,k2} \underset{\beta \rightarrow 0}{\sim} D_k(\alpha)\beta^{k+1}$  for some  $D_k(\alpha) > 0$  if  $k = 0, 2$ , and  $A_{11,12} \underset{\beta \rightarrow 0}{=} o(\beta^2)$ .

Focusing back on the Fisher information matrix expression, it comes

$$\det I(\theta) \underset{\beta \rightarrow 0}{=} \frac{D_0(\alpha)D_2(\alpha)}{\alpha^4\beta^2} + o\left(\frac{1}{\beta^2}\right).$$

Finally, we obtain:

$$J(\theta) \underset{\beta \rightarrow 0}{\sim} \frac{D'(\alpha)}{\beta}, \quad (\text{B.15})$$

where  $D'(\alpha) > 0$  is a constant independent of  $\beta$ .

### Appendix B.2.3. Proof of proposition 3

We remind firstly the asymptotic expansion of the erf function in 0:

$$\text{erf}(\gamma) \underset{\gamma \rightarrow 0}{=} \frac{2}{\sqrt{\pi}}\gamma + O(\gamma^2),$$

which allows us to state the behavior of  $\Phi(\gamma)$  when  $\gamma \rightarrow 0$ :

$$\Phi(\gamma) \underset{\gamma \rightarrow 0}{=} \frac{1}{2} + \frac{1}{\sqrt{2\pi}}\gamma + O(\gamma^2).$$

We now fix  $\alpha > 0$  and consider  $A_{k1,k2} = A_{k1} + A_{k2}$ :

$$A_{k1,k2} = \int_{-\infty}^{\infty} \tilde{F}_{A_{k1,k2}}(x) dx,$$

$$\tilde{F}_{A_{k1,k2}}(x) = \frac{x^k}{2\sqrt{\pi^3\sigma^2}} \frac{e^{-\frac{x^2}{\beta^2}} e^{-\frac{(x-\mu+\log \alpha)^2}{2\sigma^2}}}{\Phi(\beta^{-1}x)(1-\Phi(\beta^{-1}x))}.$$

We note the convergence of  $\tilde{F}_{A_{k1,k2}}(x)$  towards an integrable function when  $\beta \rightarrow \infty$ . Moreover, lemma 1 allows us to bound  $\tilde{F}_{A_{k1,k2}}$  as

$$|\tilde{F}_{A_{k1,k2}}(x)| \leq \frac{2|x|^k}{\sqrt{\pi^3\sigma^2}} e^{-\frac{(x-\mu+\log \alpha)^2}{2\sigma^2}} e^{\frac{x^2}{\beta^2}} \leq \frac{2|x|^k}{\sqrt{\pi^3\sigma^2}} e^{-\frac{(x^2-2(\mu-\log \alpha)x)^2}{4\sigma^2}} e^{\frac{(\mu+\log \alpha)^2}{2\sigma^2}},$$

for any  $x \in \mathbb{R}$  and  $\beta > 2\sigma/\sqrt{\pi}$ . This dominating function is integrable on  $\mathbb{R}$ . Thus,  $A_{k1,k2}$  admits a limit when  $\beta \rightarrow \infty$  expressed by:

$$\lim_{\beta \rightarrow \infty} A_{k1,k2} = E_k(\alpha) = \int_{-\infty}^{\infty} \frac{2x^k}{\sqrt{\pi^3\sigma^2}} e^{-\frac{(x-\mu+\log \alpha)^2}{2\sigma^2}} dx = \frac{2\sqrt{2}}{\pi} \mathbb{E}[X^k],$$

with  $X \sim \mathcal{N}(\mu - \log \alpha, \sigma^2)$ .

We can now recall the expression of the Jeffreys prior:

$$J(\theta)^2 = \left| \frac{1}{\alpha^2 \beta^6} A_{01,02} A_{21,22} - \frac{1}{\alpha^2 \beta^6} A_{11,12}^2 \right|,$$

we deduce that it is equivalent to  $(E_0(\alpha)E_2(\alpha) - E_1^2(\alpha))/\alpha^2 \beta^6$  when  $\beta \rightarrow \infty$ . Finally,

$$J(\theta) \underset{\beta \rightarrow \infty}{\sim} \frac{E'}{\alpha \beta^3},$$

with  $E' = \sqrt{E_0(\alpha)E_2(\alpha) - E_1^2(\alpha)} = 2\sigma/\pi$ .

#### Appendix B.2.4. Proof of proposition 4

As a preliminary result, we use equation (B.11) to obtain

$$\Phi(\gamma)(1 - \Phi(\gamma)) \underset{|\gamma| \rightarrow \infty}{\sim} \frac{e^{-\frac{\gamma^2}{2}}}{|\gamma| \sqrt{2\pi}}. \quad (\text{B.16})$$

We consider  $A_{k1,k2} = A_{k1} + A_{k2}$ :

$$A_{k1,k2} = C' \int_0^\infty \left( \log \frac{a}{\alpha} \right)^k \frac{e^{-\frac{1}{\beta^2} \log^2 \frac{a}{\alpha}} e^{-\frac{(\log a - \mu)^2}{2\sigma^2}}}{\Phi(\beta^{-1} \log \frac{a}{\alpha}) (1 - \Phi(\beta^{-1} \log \frac{a}{\alpha}))} \frac{da}{a}.$$

denoting  $C' = \sqrt{4\pi^3 \sigma^2}^{-1}$ . By substitution

$$\nu = \log a - \frac{\sigma^2}{\sigma^2 + \beta^2} \log \alpha - \frac{\beta^2}{\sigma^2 + \beta^2} \mu = \log a - r \log \alpha - s\mu,$$

we get

$$A_{k1,k2} = C' \int_{-\infty}^\infty \hat{F}_{A_{k1,k1}}(\nu) d\nu,$$

$$\hat{F}_{A_{k1,k1}}(\nu) = (\nu + (r-1) \log \alpha + s\mu)^k \frac{e^{-\frac{(\nu+(r+1)\log \alpha+s\mu)^2}{\beta^2}} e^{-\frac{(\nu+r\log \alpha+(s-1)\mu)^2}{2\sigma^2}}}{[\Phi(1-\Phi)](h_\beta(\nu))},$$

where  $h_\beta(\nu) = \beta^{-1}(\nu + (r-1) \log \alpha + s\mu)$ . Using equation (B.16), we obtain

$$[\Phi(1-\Phi)](h_\beta(\nu)) \underset{|\log \alpha| \rightarrow \infty}{\sim} \frac{\beta e^{-\frac{(\nu+(r-1)\log \alpha+s\mu)^2}{\beta^2}}}{|\nu + (r-1) \log \alpha + s\mu| \sqrt{2\pi}}. \quad (\text{B.17})$$

Then for a clear sight of the asymptotic behavior of  $\hat{F}_{A_{k1,k2}}$  we compute

$$\begin{aligned} & -\frac{(\nu + (r-1) \log \alpha + s\mu)^2}{2\beta^2} - \frac{(\nu + r \log \alpha + (s-1)\mu)^2}{2\sigma^2} \\ &= -\left( \frac{1}{2\beta^2} + \frac{1}{2\sigma^2} \right) \nu^2 - \left( \frac{((r-1) \log \alpha + s\mu)^2}{2\beta^2} + \frac{(r \log \alpha + (s-1)\mu)^2}{2\sigma^2} \right) \\ &= -\left( \frac{1}{2\beta^2} + \frac{1}{2\sigma^2} \right) \nu^2 - \frac{(\log \alpha - \mu)^2}{2(\beta^2 + \sigma^2)}. \end{aligned} \quad (\text{B.18})$$

We expand  $\hat{F}_{k1,k2}(\nu) = \sum_{j=1}^k C_k^j (r-1)^j \log^j \alpha (\nu + s\mu)^{k-j} g(\nu) = \sum_{j=0}^k \hat{F}_{k1,k2}^{(j)}(\nu)$ , with  $g(\nu)$  defined as

$$g(\nu) = \frac{e^{-\frac{(\nu+(r+1)\log \alpha+s\mu)^2}{\beta^2}} e^{-\frac{(\nu+r\log \alpha+(s-1)\mu)^2}{2\sigma^2}}}{[\Phi(1-\Phi)](\beta^{-1}(\nu + (r-1) \log \alpha + s\mu))}.$$

The combination of equations (B.17) and (B.18) gives that the  $\hat{F}_{k1,k2}^{(j)}$ 's satisfy

$$\hat{F}_{k1,k2}^{(j)}(v) e^{\frac{(\log \alpha - \mu)^2}{2\beta^2 + 2\sigma^2}} (\log \alpha)^{-j} |\log \alpha|^{-1} \xrightarrow{|\log \alpha| \rightarrow \infty} (\sqrt{2\pi}\beta)^{-1} C_k^j (r-1)^{j+1} (v + s\mu)^{k-j} e^{-\left(\frac{1}{2\beta^2} + \frac{1}{2\sigma^2}\right)v^2}.$$

Using lemma 2 allows to additionally dominate the above function by an integrable function as

$$|\hat{F}_{k1,k2}^{(j)}(v)| e^{\frac{(\log \alpha - \mu)^2}{2\beta^2 + 2\sigma^2}} |\log \alpha|^{-j-1} \leq \frac{\sqrt{2/\pi} e^{-\left(\frac{1}{2\beta^2} + \frac{1}{2\sigma^2}\right)v^2}}{|h_\beta(v)| + \sqrt{h_\beta(v)^2 + 4}} \leq \frac{1}{\sqrt{2\pi}} e^{-\left(\frac{1}{2\beta^2} + \frac{1}{2\sigma^2}\right)v^2}.$$

Therefore, we can switch the limits and the integration, and the following results stand:

$$\begin{aligned} C'' \beta A_{01,02} e^{\frac{(\log \alpha - \mu)^2}{2\beta^2 + 2\sigma^2}} &= (1-r)G \log \alpha - s\mu G + o(1), \\ C'' \beta A_{11,12} e^{\frac{(\log \alpha - \mu)^2}{2\beta^2 + 2\sigma^2}} &= -(1-r)^2 G \log^2 \alpha - s^2 \mu^2 G + 2(1-r)s\mu G \log \alpha - G' + o(1), \\ C'' \beta A_{22,22} e^{\frac{(\log \alpha - \mu)^2}{2\beta^2 + 2\sigma^2}} &= (1-r)^3 G \log^3 \alpha - s^3 \mu^3 G - 3(1-r)^2 s\mu G \log^2 \alpha \\ &\quad + 3(1-r)s^2 \mu^2 G \log \alpha + 3(1-r)G' \log \alpha + o(1), \end{aligned}$$

with  $C'' = (C' \sqrt{2\pi})^{-1}$ ,  $G = \sigma\beta \sqrt{2\pi(\beta^2 + \sigma^2)^{-1}}$  and  $G' = G^2/2\pi$ . This way

$$\begin{aligned} C'' \alpha \beta^8 J(\theta)^2 e^{\frac{(\log \alpha - \mu)^2}{2\beta^2 + 2\sigma^2}} &= 3(r-1)^2 s^2 \mu^2 G^2 \log^2 \alpha + 3(r-1)^2 s^2 \mu^2 G^2 \log^2 \alpha \\ &\quad + 3(r-1)^2 G G' \log^2 \alpha - 4(r-1)^2 s^2 \mu^2 G^2 \log^2 \alpha \\ &\quad - 2(r-1)^2 s^2 \mu^2 G^2 \log^2 \alpha - 2(r-1)^2 G G' \log^2 \alpha + o(\log^2 \alpha). \end{aligned}$$

Notice the above equality is still valid when  $\log \alpha \rightarrow -\infty$ . Finally

$$J(\theta) \underset{|\log \alpha| \rightarrow \infty}{\sim} G''(\beta) \frac{|\log \alpha|}{\alpha} \exp\left(-\frac{(\log \alpha - \mu)^2}{2\beta^2 + 2\sigma^2}\right),$$

with

$$G''(\beta) = C''^{-1} (r-1)^2 G G' \beta^{-4} = \frac{2\sigma^3 \beta^3}{\sqrt{\pi}(\sigma^2 + \beta^2)^{7/2}}.$$

## Appendix C. A review of the posterior asymptotics within Straub and Der Kiureghian [14]'s framework

In this paper we have compared our approach with the one that results from an adaptation of the prior suggested by Straub and Der Kiureghian [14]. We proved in Appendix B that this prior gives an improper posterior in our framework. This questions the validity of the MCMC simulations, which could explain the lower performance of the SK's prior compared to Jeffreys prior. The authors in [14] use the Bayesian methodology as we do, yet the consideration of uncertainties over the observed earthquake intensity measures and the equipment capacities lead to a slightly different likelihood. To stay convinced that the drawbacks of their prior that we highlighted are not due to our statistical choices, we dedicate this section to the study of the asymptotics of the posterior in the exact framework of [14].

First we present the exact model of Straub and Der Kiureghian for the estimation of seismic fragility curves in Appendix C.1, using notations consistent with our work. Second the likelihood and its asymptotics are derived in Appendix C.2. Finally the convergence rates of the posterior are expressed in Appendix C.3 and allow us to conclude that the SK posterior is indeed improper.

### Appendix C.1. Statistical model and likelihood

We consider the observations of earthquakes labelled  $l = 1, \dots, L$  at equipments labelled  $i = 1, \dots, I_j$  located in substations labelled  $j = 1, \dots, J$ . The observed items are  $(\mathbf{z}_{jl}, \hat{a}_{jl})_{j,l}$ ,  $\mathbf{z}_{jl} = (z_{ijl})_i$  being the failure occurrences of the  $I_j$  equipments at substation  $j$  during earthquake  $l$  ( $z_{ijl} \in \{0, 1\}$ ) and  $\hat{a}_{jl}$  being the observed IM at substation  $j$  during earthquake  $l$  ( $\hat{a}_{jl} \in (0, +\infty)$ ). They are assumed to follow the latent model presented below.

At substation  $j$  the  $l$ -th earthquake results in an IM value  $a_{jl}$  that is observed with an uncertainty multiplicative noise:  $\log \hat{a}_{jl} = \log a_{jl} + \varepsilon_{jl}$  where  $\varepsilon_{jl} \sim \mathcal{N}(0, \sigma_\varepsilon^2)$ . The noise variance  $\sigma_\varepsilon^2$  is supposed to be known. The uncertain intrinsic capacity of equipment  $i$  at substation  $j$  is  $r_{ij} \sim \mathcal{N}(\mu_r, \sigma_r^2)$  and  $y_{jl} \sim \mathcal{N}(0, \sigma_y^2)$  is the uncertain factor common to all equipment capacities at substation  $j$  during earthquake  $l$ . The random variables  $r_{ij}$ ,  $y_{jl}$  and  $\varepsilon_{jl}$  are supposed to be independent.

A failure for equipment  $i$  at substation  $j$  during earthquake  $l$  is considered when the performance of the structural component  $g_{ijl}$  satisfies  $g_{ijl} > 0$ . This performance can be expressed as

$$g_{ijl} = \log \hat{a}_{jl} + \varepsilon_{jl} - y_{jl} - r_{ij} = x_{jl} - r_{ij} \quad \text{with } x_{jl} = \log \hat{a}_{jl} + \varepsilon_{jl} - y_{jl}.$$

This states the following conditional relation between the observed data:

$$p(z_{ijl}|\hat{a}_{jl}, \Sigma) = \int_{\mathbb{R}} p(z_{ijl}|x_{jl}, \hat{a}_{jl}, \Sigma) \frac{\exp\left(-\frac{(x_{jl} - \log \hat{a}_{jl})^2}{2(\sigma_\varepsilon^2 + \sigma_y^2)}\right)}{\sqrt{2\pi(\sigma_\varepsilon^2 + \sigma_y^2)}} dx_{jl}, \quad (\text{C.1})$$

denoting  $\Sigma = (\sigma_r, \sigma_y, \mu_r)$ , and with

$$p(z_{ijl}|x_{jl}, \hat{a}_{jl}, \Sigma) = \Phi\left(\frac{x_{jl} - \mu_r}{\sigma_r}\right)^{z_{ijl}} \left(1 - \Phi\left(\frac{x_{jl} - \mu_r}{\sigma_r}\right)\right)^{1-z_{ijl}}, \quad (\text{C.2})$$

when substation  $j$  is affected only by one earthquake. Indeed, the method proposed in [14] considers the cases in which a substation may be affected by two successive earthquakes and takes into account the fact that its response to the second is correlated to its response to the first one. That would lead to a different likelihood. However, it is mentioned that this possibility concerns only a few data-items. We, therefore, limit our calculations to the simplest case and we assume  $l = L = 1$ , we thus drop the subscript  $l$  in what follows.

Finally, the likelihood for this model can be expressed as:

$$\ell_J(\mathbf{z}|\hat{\mathbf{a}}, \Sigma) = \prod_{j=1}^J \int_{\mathbb{R}} \prod_{i=1}^{I_j} p(z_{ij}|x_j, \log \hat{a}_j, \Sigma) \frac{\exp\left(-\frac{(x_j - \log \hat{a}_j)^2}{2(\sigma_\varepsilon^2 + \sigma_y^2)}\right)}{\sqrt{2\pi(\sigma_\varepsilon^2 + \sigma_y^2)}} dx_j, \quad (\text{C.3})$$

denoting  $\mathbf{z} = (\mathbf{z}_j)_{j=1}^J$ ,  $\hat{\mathbf{a}} = (\hat{a}_j)_{j=1}^J$ , and with the integrated conditional distribution being defined in equation (C.2).

In the Bayesian framework introduced in [14] the model parameter is  $\Sigma$ . We denote  $\alpha = \exp \mu_r$ ,  $\beta = \sqrt{\sigma_r^2 + \sigma_y^2}$  and  $\rho = \sigma_y^2 / \beta^2$ . Therefore, denoting  $\theta = (\alpha, \beta, \rho)$ , the knowledge of  $\Sigma$  becomes equivalent to the one of  $\theta$  and the likelihood of equation (C.3) can be expressed conditionally to  $\theta$  instead of  $\Sigma$ :

$$\ell_J(\mathbf{z}|\hat{\mathbf{a}}, \theta) = \prod_{j=1}^J \int_{\mathbb{R}} \prod_{i=1}^{I_j} \Psi^{z_{ij}}\left(\frac{x - \log \alpha}{\beta \sqrt{1 - \rho}}\right) \frac{\exp\left(-\frac{(x - \log \alpha)^2}{2(\sigma_\varepsilon^2 + \rho\beta^2)}\right)}{\sqrt{2\pi(\sigma_\varepsilon^2 + \rho\beta^2)}} dx, \quad (\text{C.4})$$

where the notation  $\Psi^{z_{ij}}(\gamma)$  is used to denote  $\Phi(\gamma)^{z_{ij}}(1 - \Phi(\gamma))^{1-z_{ij}}$ .

[Straub and Der Kiureghian](#) propose the following improper prior distribution for the parameter  $\theta$ :

$$\pi_{SK}(\theta) \propto \frac{1}{\beta\alpha} \exp\left(-\frac{(\log \alpha - \mu)^2}{2\sigma^2}\right) \mathbb{1}_{0 \leq \rho \leq 1}. \quad (\text{C.5})$$

*A posteriori* estimations of  $\theta$  are consequently generated from MCMC simulations of the posterior distribution

$$p(\theta|\mathbf{z}, \hat{\mathbf{a}}) \propto \ell_J(\mathbf{z}|\hat{\mathbf{a}}, \theta) \pi_{SK}(\theta). \quad (\text{C.6})$$

### Appendix C.2. Likelihood asymptotics

In this appendix we study the asymptotics of the likelihood defined in (C.4) when  $\beta \rightarrow \infty$ . First we consider the substitution  $u = (x - \log \hat{a}_j) / \sqrt{\sigma_\varepsilon^2 + \rho\beta^2}$  to express the likelihood as

$$\begin{aligned} \ell_J(\mathbf{z}|\hat{\mathbf{a}}, \theta) &= \prod_{j=1}^J \int_{\mathbb{R}} f_j^\beta(u) du, \\ f_j^\beta(u) &= \prod_{i=1}^{I_j} \Phi(h_j^\beta(u))^{z_{ij}} (1 - \Phi(h_j^\beta(u)))^{1-z_{ij}} \frac{e^{-\frac{u^2}{2}}}{\sqrt{2\pi}}, \end{aligned}$$

with

$$h_j^\beta(u) = \frac{(u + \log \hat{a}_j) \sqrt{\sigma_\varepsilon^2 + \rho\beta^2} - \log \alpha}{\beta \sqrt{1 - \rho}}.$$

This way, reminding  $0 \leq \Phi(1 - \Phi) \leq 1$ ,  $f_j^\beta$  can be dominated for any  $\beta, u$  by  $u \mapsto e^{-u^2/2} / \sqrt{2\pi}$  and it converges as  $\beta \rightarrow +\infty$  as follows:

$$\lim_{\beta \rightarrow \infty} f_j^\beta(u) = \prod_{i=1}^{I_j} \Psi^{z_{ij}} \left( \frac{(u + \log \hat{a}_j) \sqrt{\rho}}{\sqrt{1 - \rho}} \right) \frac{e^{-\frac{u^2}{2}}}{\sqrt{2\pi}}.$$

This gives the following limit for the likelihood:

$$\lim_{\beta \rightarrow \infty} \ell_J(\mathbf{z}|\hat{\mathbf{a}}, \theta) = \prod_{j=1}^J \int_{\mathbb{R}} \prod_{i=1}^{I_j} \Psi^{z_{ij}} \left( \frac{(u + \log \hat{a}_j) \sqrt{\rho}}{\sqrt{1 - \rho}} \right) \frac{e^{-\frac{u^2}{2}}}{\sqrt{2\pi}} du, \quad (\text{C.7})$$

which is a positive quantity.

### Appendix C.3. Posterior asymptotics

By combining equations (C.7), (C.6) and (C.5) we find the posterior asymptotics

$$p(\theta|\mathbf{z}, \hat{\mathbf{a}}) \underset{\beta \rightarrow \infty}{\sim} \frac{C}{\beta}, \quad (\text{C.8})$$

with  $C$  being a positive constant. This makes the posterior improper w.r.t.  $\beta$ , with the same convergence rate as the one that was derived in our framework.

## References

- [1] R. P. Kennedy, C. A. Cornell, R. D. Campbell, S. J. Kaplan, F. Harold, Probabilistic seismic safety study of an existing nuclear power plant, *Nuclear Engineering and Design* 59 (1980) 315–338. doi:10.1016/0029-5493(80)90203-4.
- [2] R. P. Kennedy, M. K. Ravindra, Seismic fragilities for nuclear power plant risk studies, *Nuclear Engineering and Design* 79 (1984) 47–68. doi:10.1016/0029-5493(84)90188-2.
- [3] Y.-J. Park, C. H. Hofmayer, N. C. Chokshi, Survey of seismic fragilities used in PRA studies of nuclear power plants, *Reliability Engineering & System Safety* 62 (1998) 185–195. doi:10.1016/S0951-8320(98)00019-2.
- [4] R. P. Kennedy, Risk based seismic design criteria, *Nuclear Engineering and Design* 192 (1999) 117–135. doi:10.1016/S0029-5493(99)00102-8.
- [5] C. A. Cornell, Hazard, ground motions and probabilistic assessments for PBSA, in: *Proceedings of the International Workshop on Performance-Based Seismic Design - Concepts and Implementation*, PEER Center, University of California, Berkeley, 2004, pp. 39–52.
- [6] M. D. Grigoriu, A. Radu, Are seismic fragility curves fragile?, *Probabilistic Engineering Mechanics* 63 (2021) 103115. doi:10.1016/j.probengmech.2020.103115.
- [7] *Proceedings of the International Workshop on Performance-Based Seismic Design - Concepts and Implementation*, PEER Report 2004-05, PEER Center, University of California, Berkeley, 2004.
- [8] K. Porter, R. P. Kennedy, R. Bachman, Creating fragility functions for performance-based earthquake engineering, *Earthquake Spectra* 23 (2007) 471–489. doi:10.1193/1.2720892.
- [9] P. Gardoni, A. Der Kiureghian, K. M. Mosalam, Probabilistic capacity models and fragility estimates for reinforced concrete columns based on experimental observations, *Journal of Engineering Mechanics* 128 (2002) 1024–1038. doi:10.1061/(ASCE)0733-9399(2002)128:10(1024).

- [10] I. Zentner, M. Gündel, N. Bonfils, Fragility analysis methods: Review of existing approaches and application, *Nuclear Engineering and Design* 323 (2017) 245–258. doi:10.1016/j.nucengdes.2016.12.021.
- [11] D.-E. Choe, P. Gardoni, D. Rosowsky, Closed-form fragility estimates, parameter sensitivity, and bayesian updating for rc columns, *Journal of Engineering Mechanics* 133 (2007) 833–843. doi:10.1061/(ASCE)0733-9399(2007)133:7(833).
- [12] M. Shinozuka, M. Q. Feng, J. Lee, T. Naganuma, Statistical analysis of fragility curves, *Journal of Engineering Mechanics* 126 (2000) 1224–1231. doi:10.1061/(ASCE)0733-9399(2000)126:12(1224).
- [13] D. Lallemand, A. Kiremidjian, H. Burton, Statistical procedures for developing earthquake damage fragility curves, *Earthquake Engineering & Structural Dynamics* 44 (2015) 1373–1389. doi:10.1002/eqe.2522.
- [14] D. Straub, A. Der Kiureghian, Improved seismic fragility modeling from empirical data, *Structural Safety* 30 (2008) 320–336. doi:10.1016/j.strusafe.2007.05.004.
- [15] I. Zentner, Numerical computation of fragility curves for NPP equipment, *Nuclear Engineering and Design* 240 (2010) 1614–1621. doi:10.1016/j.nucengdes.2010.02.030.
- [16] F. Wang, C. Feau, Influence of Input Motion’s Control Point Location in Nonlinear SSI Analysis of Equipment Seismic Fragilities: Case Study on the Kashiwazaki-Kariwa NPP, *Pure and Applied Geophysics* (2020). doi:10.1016/j.engstruct.2018.02.024.
- [17] T. K. Mandal, S. Ghosh, N. N. Pujari, Seismic fragility analysis of a typical indian PHWR containment: Comparison of fragility models, *Structural Safety* 58 (2016) 11–19. doi:10.1016/j.strusafe.2015.08.003.
- [18] Z. Wang, N. Pedroni, I. Zentner, E. Zio, Seismic fragility analysis with artificial neural networks: Application to nuclear power plant equipment, *Engineering Structures* 162 (2018) 213–225. doi:10.1016/j.engstruct.2018.02.024.
- [19] Z. Wang, I. Zentner, E. Zio, A Bayesian framework for estimating fragility curves based on seismic damage data and numerical simulations by adaptive neural networks, *Nuclear Engineering and Design* 338 (2018) 232–246. doi:10.1016/j.nucengdes.2018.08.016.
- [20] C. Zhao, N. Yu, Y. Mo, Seismic fragility analysis of AP1000 SB considering fluid-structure interaction effects, *Structures* 23 (2020) 103–110. doi:10.1016/j.istruc.2019.11.003.
- [21] B. R. Ellingwood, Earthquake risk assessment of building structures, *Reliability Engineering & System Safety* 74 (2001) 251–262. doi:10.1016/S0951-8320(01)00105-3.
- [22] S.-H. Kim, M. Shinozuka, Development of fragility curves of bridges retrofitted by column jacketing, *Probabilistic Engineering Mechanics* 19 (2004) 105–112. doi:10.1016/j.probenmech.2003.11.009, fourth International Conference on Computational Stochastic Mechanics.
- [23] C. Mai, K. Konakli, B. Sudret, Seismic fragility curves for structures using non-parametric representations, *Frontiers of Structural and Civil Engineering* 11 (2017) 169–186. doi:10.1007/s11709-017-0385-y.
- [24] K. Trevelopoulos, C. Feau, I. Zentner, Parametric models averaging for optimized non-parametric fragility curve estimation based on intensity measure data clustering, *Structural Safety* 81 (2019) 101865. doi:10.1016/j.strusafe.2019.05.002.
- [25] Y. Katayama, Y. Ohtori, T. Sakai, H. Muta, Bayesian-estimation-based method for generating fragility curves for high-fidelity seismic probability risk assessment, *Journal of Nuclear Science and Technology* 58 (2021) 1220–1234. doi:10.1080/00223131.2021.1931517.
- [26] C. Bernier, J. E. Padgett, Fragility and risk assessment of aboveground storage tanks subjected to concurrent surge, wave, and wind loads, *Reliability Engineering & System Safety* 191 (2019) 106571. doi:10.1016/j.res.2019.106571.
- [27] J. Kiani, C. Camp, S. Pezeshk, On the application of machine learning techniques to derive seismic fragility curves, *Computers & Structures* 218 (2019) 108–122. doi:10.1016/j.compstruc.2019.03.004.
- [28] R. Sainct, C. Feau, J.-M. Martinez, J. Garnier, Efficient methodology for seismic fragility curves estimation by active learning on support vector machines, *Structural Safety* 86 (2020) 101972. doi:10.1016/j.strusafe.2020.101972.
- [29] I. Gidaris, A. A. Taflanidis, G. P. Mavroedidis, Kriging metamodeling in seismic risk assessment based on stochastic ground motion models, *Earthquake Engineering & Structural Dynamics* 44 (2015) 2377–2399. doi:10.1002/eqe.2586.
- [30] R. Gentile, C. Galasso, Gaussian process regression for seismic fragility assessment of building portfolios, *Structural Safety* 87 (2020) 101980. doi:10.1016/j.strusafe.2020.101980.
- [31] C. Gauchy, C. Feau, J. Garnier, Uncertainty quantification and global sensitivity analysis of seismic fragility curves using kriging, Submitted to *International Journal for Uncertainty Quantification* (2022). doi:10.48550/ARXIV.2210.06266.
- [32] C. Mai, M. D. Spiridonakos, E. Chatzi, B. Sudret, Surrogate modeling for stochastic dynamical systems by combining nonlinear autoregressive with exogenous input models and polynomial chaos expansions, *International Journal for Uncertainty Quantification* 6 (2016) 313–339. doi:10.1615/Int.J.UncertaintyQuantification.2016016603.
- [33] C. C. Mitropoulou, M. Papadrakakis, Developing fragility curves based on neural network IDA predictions, *Engineering Structures* 33 (2011) 3409–3421. doi:10.1016/j.engstruct.2011.07.005.
- [34] C. Gauchy, C. Feau, J. Garnier, Importance sampling based active learning for parametric seismic fragility curve estimation, Submitted to *Reliability Engineering & System Safety* (2021). doi:10.48550/ARXIV.2109.04323.
- [35] P. S. Koutsourelakis, Assessing structural vulnerability against earthquakes using multi-dimensional fragility surfaces: A Bayesian framework, *Probabilistic Engineering Mechanics* 25 (2010) 49–60. doi:10.1016/j.probenmech.2009.05.005.
- [36] G. Damblin, M. Keller, A. Pasanisi, P. Barbillon, É. Parent, Approche décisionnelle bayésienne pour estimer une courbe de fragilité, *Journal de la Société Française de Statistique* 155 (2014) 78–103. URL: <https://hal.archives-ouvertes.fr/hal-01545648>.
- [37] S. K. Tadinada, A. Gupta, Structural fragility of t-joint connections in large-scale piping systems using equivalent elastic time-history simulations, *Structural Safety* 65 (2017) 49–59. doi:10.1016/j.strusafe.2016.12.003.
- [38] S. Kwag, A. Gupta, Computationally efficient fragility assessment using equivalent elastic limit state and Bayesian updating, *Computers & Structures* 197 (2018) 1–11. doi:10.1016/j.compstruc.2017.11.011.
- [39] J.-S. Jeon, S. Mangalathu, J. Song, R. Desroches, Parameterized seismic fragility curves for curved multi-frame concrete box-girder bridges using bayesian parameter estimation, *Journal of Earthquake Engineering* 23 (2019) 954–979. doi:10.1080/13632469.2017.1342291.
- [40] A. Tabandeh, P. Asem, P. Gardoni, Physics-based probabilistic models: Integrating differential equations and observational data, *Structural Safety* 87 (2020) 101981. doi:10.1016/j.strusafe.2020.101981.
- [41] R. E. Kass, L. Wasserman, The selection of prior distributions by formal rules, *Journal of the American Statistical Association* 91 (1996) 1343–1370. doi:10.1080/01621459.1996.10477003.

- [42] J. O. Berger, J. M. Bernardo, D. Sun, The formal definition of reference priors, *The Annals of statistics* 37 (2009) 905–938. doi:[10.1214/07-AOS587](https://doi.org/10.1214/07-AOS587).
- [43] C. Robert, *The Bayesian Choice*, Texts in Statistics, 2 ed., Springer, 2007.
- [44] J. M. Bernardo, Reference posterior distributions for Bayesian inference, *Journal of the Royal Statistical Society. Series B* 41 (1979) 113–147. doi:[10.1111/j.2517-6161.1979.tb01066.x](https://doi.org/10.1111/j.2517-6161.1979.tb01066.x).
- [45] E. T. Jaynes, On the rationale of maximum-entropy methods, *Proceedings of the IEEE* 70 (1982) 939–952. doi:[10.1109/PROC.1982.12425](https://doi.org/10.1109/PROC.1982.12425).
- [46] B. S. Clarke, A. R. Barron, Jeffreys’ prior is asymptotically least favorable under entropy risk, *Journal of Statistical Planning and Inference* 41 (1994) 37–60. doi:[10.1016/0378-3758\(94\)90153-8](https://doi.org/10.1016/0378-3758(94)90153-8).
- [47] J. M. Bernardo, Reference analysis, in: *Bayesian Thinking*, volume 25 of *Handbook of Statistics*, Elsevier, 2005, pp. 17–90. doi:[https://doi.org/10.1016/S0169-7161\(05\)25002-2](https://doi.org/10.1016/S0169-7161(05)25002-2).
- [48] S. Rezaeian, *Stochastic Modeling and Simulation of Ground Motions for Performance-Based Earthquake Engineering*, Ph.D. thesis, University of California, Berkeley, 2010.
- [49] H. Haario, E. Saksman, J. Tamminen, An adaptive metropolis algorithm, *Bernoulli* 7 (2001) 223–242. doi:[10.2307/3318737](https://doi.org/10.2307/3318737).
- [50] P. Gehl, J. Douglas, D. M. Seyed, Influence of the number of dynamic analyses on the accuracy of structural response estimates, *Earthquake Spectra* 31 (2015) 97–113. doi:[10.1193/102912EQS320M](https://doi.org/10.1193/102912EQS320M).
- [51] J. W. Baker, Efficient analytical fragility function fitting using dynamic structural analysis, *Earthquake Spectra* 31 (2015) 579–599. doi:[10.1193/021113EQS025M](https://doi.org/10.1193/021113EQS025M).
- [52] A. van der Vaart, *Asymptotic statistics*, Cambridge Series in Statistical and Probabilistic Mathematics, 1 ed., Cambridge University Press, 1992.
- [53] F. Touboul, P. Sollogoub, N. Blay, Seismic behaviour of piping systems with and without defects: experimental and numerical evaluations, *Nuclear Engineering and Design* 192 (1999) 243–260. doi:[10.1016/S0029-5493\(99\)00111-9](https://doi.org/10.1016/S0029-5493(99)00111-9).
- [54] CEA, CAST3M, 2019. URL: <http://www-cast3m.cea.fr/>.
- [55] F. Touboul, N. Blay, P. Sollogoub, S. Chapuliot, Enhanced seismic criteria for piping, *Nuclear Engineering and Design* 236 (2006) 1–9. doi:[10.1016/j.nucengdes.2005.07.002](https://doi.org/10.1016/j.nucengdes.2005.07.002).
- [56] D. Beylat, *Contribution à l’étude du comportement dynamique aléatoire de structures libres et empilées sous séisme*, Theses, Université Clermont Auvergne [2017-2020], 2020. URL: <https://theses.hal.science/tel-03159237>.
- [57] J. T. Chu, On bounds for the normal integral, *Biometrika* 42 (1955) 263–265. doi:[10.2307/2333443](https://doi.org/10.2307/2333443).
- [58] K. Ito, H. P. McKean, *Diffusion processes and their sample paths*, Springer-Verlag, Berlin, 1974.